

Sparse Cholesky factorization by Kullback-Leibler minimization

Florian Schäfer*

Matthias Katzfuss†

Houman Owhadi‡

December 22, 2024

Abstract

Abstract: We propose to compute a sparse approximate inverse Cholesky factor L of a dense covariance matrix Θ by minimizing the Kullback-Leibler divergence between the Gaussian distributions $\mathcal{N}(0, \Theta)$ and $\mathcal{N}(0, L^{-\top} L^{-1})$, subject to a sparsity constraint. Surprisingly, this problem has a closed-form solution that can be computed efficiently, recovering the popular Vecchia approximation in spatial statistics. Based on recent results on the approximate sparsity of inverse Cholesky factors of Θ obtained from pairwise evaluation of Green’s functions of elliptic boundary-value problems at points $\{x_i\}_{1 \leq i \leq N} \subset \mathbb{R}^d$, we propose an elimination ordering and sparsity pattern that allows us to compute ϵ -approximate inverse Cholesky factors of such Θ in computational complexity $\mathcal{O}(N \log(N/\epsilon)^d)$ in space and $\mathcal{O}(N \log(N/\epsilon)^{2d})$ in time. To the best of our knowledge, this is the best asymptotic complexity for this class of problems. Furthermore, our method is embarrassingly parallel, automatically exploits low-dimensional structure in the data, and can perform Gaussian-process regression in linear (in N) space complexity. Motivated by the optimality properties of our methods, we propose methods for applying it to the joint covariance of training and prediction points in Gaussian-process regression, greatly improving stability and computational cost. Finally, we show how to apply our method to the important setting of Gaussian processes with additive noise, sacrificing neither accuracy nor computational complexity.

Keywords: covariance function, Vecchia approximation, kernel matrix, sparsity, transport map, factorized sparse approximate inverse.

2010 Mathematics Subject Classification: 65F30 (42C40, 65F50, 65N55, 65N75, 60G42, 68W40)

1 Introduction

The problem: This work is concerned with the sparse inverse–Cholesky factorization of large dense positive-definite matrices $\Theta \in \mathbb{R}^{N \times N}$, frequently arising as *kernel matrices* in machine-learning methods using the “kernel trick” (Hofmann et al., 2008), as *covariance matrices* in Gaussian-process (GP) statistics (e.g., Rasmussen and Williams, 2006), and as *Green’s matrices* in the numerical analysis of elliptic partial differential equations (PDEs). Naive computations of quantities such as Θv , $\Theta^{-1}v$, $\log \det \Theta$, which are required by the applications mentioned above, scale as $\mathcal{O}(N^2)$ or $\mathcal{O}(N^3)$, and become prohibitively expensive for $N > 10^5$ on present-day hardware.

*California Institute of Technology, MC 305-16, 1200 East California Boulevard, Pasadena, CA 91125, USA, florian.schaefer@caltech.edu, Phone: (626) 395-3531, Fax: (626) 578-0124, Corresponding Author

†Department of Statistics, Texas A&M University

‡California Institute of Technology

Existing work: Numerous approaches have been proposed in the literature to improve this computational complexity by taking advantage of the structure of Θ . Many rely on sparse approximations to the kernel matrix (e.g., Furrer et al., 2006; Kaufman et al., 2008), its inverse (e.g., Lindgren et al., 2011; Roininen et al., 2011, 2013, 2014), or the Cholesky factor of its inverse (e.g., Vecchia, 1988); also popular are low-rank approximations (e.g., Williams and Seeger, 2001; Smola and Bartlett, 2001; Fine and Scheinberg, 2001; Bach and Jordan, 2003; Fowlkes et al., 2004; Banerjee et al., 2008) and combinations of low-rank and sparse approximations (e.g., Schwaighofer and Tresp, 2003; Snelson and Ghahramani, 2006; Quiñonero-Candela and Rasmussen, 2005; Sang and Huang, 2012). Near-linear computational complexity can be achieved by applying these mechanisms hierarchically on multiple scales. Examples of hierarchical sparse approximations include wavelet methods (e.g., Beylkin et al., 1991), the multi-resolution approximation (Katzfuss, 2016; Katzfuss and Gong, 2019), and (implicitly) some versions of the Vecchia approximation (Katzfuss and Guinness, 2019). Hierarchical application of low-rank approximations leads to *hierarchical matrices* (Hackbusch, 1999; Hackbusch and Khoromskij, 2000; Hackbusch and Börm, 2002; Chandrasekaran et al., 2004; Ambikasaran and Darve, 2013; Ho and Ying, 2016), which are an algebraic abstraction of the fast multipole method (Greengard and Rokhlin, 1987). Schäfer et al. (2017) proposed an approximation based on incomplete Cholesky factorization that can be interpreted as both hierarchical sparse and hierarchical low-rank.

The best asymptotic (in N and ϵ) memory complexity for the ϵ -accurate compression of an $N \times N$ kernel matrix with finitely smooth covariance function and d -dimensional feature space is $\mathcal{O}(N \log^d(N/\epsilon))$, which is achieved by wavelets in nonstandard form (Beylkin et al., 1991, for asymptotically smooth kernels), or sparse inverse Cholesky factors of Θ (Schäfer et al., 2017, based on results in Owhadi and Scovel, 2017, 2019). However, we are not aware of *practical* algorithms that provably compute such approximations in near-linear time from¹ $\mathcal{O}(N \log^d(N/\epsilon))$ entries of Θ chosen a priori.

Our method: We propose to compute a sparse approximate inverse Cholesky factor L of Θ , by minimizing with respect to L subject to a sparsity constraint, the Kullback-Leibler (KL) divergence between two centered multivariate normal distributions with covariance matrices Θ and $(LL^\top)^{-1}$. Surprisingly, this minimization problem has a closed-form solution, enabling the efficient computation of optimally accurate Cholesky factors for any specified sparsity pattern.

The resulting approximation can be shown to be equivalent to the Vecchia approximation of Gaussian processes (Vecchia, 1988), which has become very popular for the analysis of geospatial data (e.g., Stein et al., 2004; Datta et al., 2016; Sun and Stein, 2016; Guinness, 2018; Katzfuss and Guinness, 2019; Katzfuss et al., 2018); to the best of our knowledge, rigorous convergence rates and error bounds were previously unavailable for Vecchia approximations, and this work is the first one presenting such results. An equivalent approximation has also been proposed by Kaporin (1990) and Kolotilina and Yeremin (1993) in the literature on factorized sparse approximate inverse (FSAI) preconditioners of (typically) sparse matrices (see Benzi and Tuma, 1999, for a review and comparison); however, its KL-divergence optimality has not been observed before. KL-minimization has also been used to obtain sparse lower-triangular transport maps by Marzouk et al. (2017); while this literature is mostly concerned with the efficient sampling of non-Gaussian probability measures, the present work shows that an analogous approach can be used to obtain fast algorithms for numerical linear algebra, if the sparsity pattern is chosen appropriately.

¹Hidden constants in all asymptotic complexities may depend on the dimension d of the dataset.

State-of-the-art computational complexity: The computational complexity and approximation accuracy of our approach depend on the choice of elimination ordering and sparsity pattern. We propose a particular choice, similar to Guinness (2018) and Schäfer et al. (2017), that is motivated by the *screening effect* (e.g., Stein, 2002, 2011), which implies (approximate) conditional independence for many kernels of common interest. By using a grouping algorithm similar to the heuristics proposed by Ferronato et al. (2015) and Guinness (2018), we can show that the approximate inverse Cholesky factor can be computed in computational complexity $\mathcal{O}(N\rho^{2d})$ in time and $\mathcal{O}(N\rho^d)$ in space, using only $\mathcal{O}(N\rho^d)$ entries of the original kernel matrix Θ , where ρ is a tuning parameter trading accuracy for computational efficiency.

Schäfer et al. (2017) observe that recent results on numerical homogenization and operator-adapted wavelets (Målqvist and Peterseim, 2014; Kornhuber and Yserentant, 2016; Owhadi and Scovel, 2017) imply the exponential decay of the inverse Cholesky factors of Θ , if the kernel function is the Green’s function of an elliptic boundary-value problem. Using these results, we prove that in this setting, an ϵ -approximation of Θ can be obtained by choosing $\rho \approx \log(N/\epsilon)$. This leads to the best known trade-off between computational complexity and accuracy for this class of kernel matrices.

Practical advantages: Our method has important *practical* advantages complementing its theoretical and asymptotic properties. In many GP regression applications, large values of ρ are computationally intractable with present-day resources. By incorporating prediction points in the computation of KL-optimal inverse-Cholesky factors, we obtain a GP regression algorithm that remains accurate for small (≈ 3) values of ρ . Remarkably, this approach is more accurate than directly truncating the *true* Cholesky factor of Θ^{-1} to the same sparsity pattern, or than computing the inverse Cholesky factors without the prediction points.

For other hierarchy-based methods, the computational complexity depends exponentially on the dimension d of the dataset. In contrast, because the construction of the ordering and sparsity pattern only uses pairwise distances between points, our algorithms automatically adapt to low-dimensional structure in the data, and operate in complexities identified by replacing d with the *intrinsic dimension* $\tilde{d} \leq d$ of the dataset.

An important limitation of existing methods based on the screening effect (Guinness, 2018; Schäfer et al., 2017; Katzfuss et al., 2018) is that they deteriorate when applied to independent sums of two GPs, such as when combining a GP with additive Gaussian white noise. Extending ideas proposed in Schäfer et al. (2017), we are able to fully preserve both the accuracy and asymptotic complexity of our method over a wide range of noise levels. To the best of our knowledge, this is the first time this has been achieved by a method based on the screening effect.

Finally, our algorithm is intrinsically parallel, because it allows each column of the sparse factor to be computed independently (as in the setting of the Vecchia approximation, factorized sparse approximate inverses, and lower-triangular transport maps). Furthermore, we show that in the context of GP regression, the loglikelihood, the posterior mean, and the posterior variance can be computed in $\mathcal{O}(N + \rho^{\tilde{d}})$ space complexity. In a parallel setting, we require $\mathcal{O}(\rho^d)$ communication between the different workers for every $\mathcal{O}(\rho^{3d})$ floating point operations, resulting in a total communication complexity of $\mathcal{O}(N)$. Here, most of the floating point operations arise from calls to highly optimized BLAS and LAPACK routines.

Outline: The remainder of this article is organized as follows. In Section 2, we show how sparsity-constrained KL-minimization yields a simple formula for approximating the inverse Cholesky factor of a positive-definite matrix. In Section 3, we present elimination orderings and sparsity patterns that provably lead to state-of-the-art trade-off between computational complexity and accuracy

when applied to Green’s functions of elliptic PDEs, and that we recommend more generally for covariance matrices of Gaussian processes that are subject to a screening effect. In Section 3.3, we bound the computational complexity of our algorithm in terms of the intrinsic dimension of the dataset, and rigorously quantify its complexity/accuracy trade-off. In Section 4, we showcase three extensions of our method, allowing the treatment of additive noise due to measurement errors, improving the speed and accuracy of prediction, and enabling GP regression at *linear* complexity in space and communication (between workers) in a distributed setting. In Section 5, we present numerical experiments applying our method to GP regression and to boundary-element methods for the solution of elliptic PDEs. We summarize our findings in Section 6. Proofs and further implementation details are deferred to an appendix.

2 Cholesky factorization by KL-minimization

The Kullback-Leibler divergence between two probability measures P and Q is defined as $D_{\text{KL}}(P \parallel Q) = \int \log(dP/dQ) dP$. If Q is an approximation of P , then the KL divergence is the expected difference between the associated true and approximate log-densities, and so its minimization is directly relevant for accurate approximations of GP inference, including GP prediction and likelihood-based inference on hyperparameters. By virtue of its connection to the likelihood ratio test (Eguchi and Copas, 2006), the KL divergence can also be interpreted as the strength of the evidence that samples from P were not instead obtained from Q . If P and Q are both N -variate centered normal distributions, the KL divergence is equivalent to a popular loss function for covariance-matrix estimation (James and Stein, 1961), and it can be written as

$$2 D_{\text{KL}}(\mathcal{N}(0, \Theta_1) \parallel \mathcal{N}(0, \Theta_2)) = \text{trace}(\Theta_2^{-1}\Theta_1) + \log\det(\Theta_2) - \log\det(\Theta_1) - N. \quad (2.1)$$

Let Θ be a positive-definite matrix of size $N \times N$. Given a lower-triangular sparsity set $S \subset I \times I$, where $I = \{1, \dots, N\}$, we want to use

$$L := \operatorname{argmin}_{\hat{L} \in \mathcal{S}} D_{\text{KL}}\left(\mathcal{N}(0, \Theta) \parallel \mathcal{N}(0, (\hat{L}\hat{L}^\top)^{-1})\right) \quad (2.2)$$

as an approximate Cholesky factor for Θ^{-1} , where $\mathcal{S} := \{A \in \mathbb{R}^{N \times N} : A_{ij} \neq 0 \Rightarrow (i, j) \in S\}$. While solving the non-quadratic program (2.2) might seem challenging, it turns out that it has a closed-form solution that can be computed efficiently:

Theorem 2.1. *The nonzero entries of the i -th column of L as defined in Equation (2.2) are given by*

$$L_{s_i, i} = \frac{\Theta_{s_i, s_i}^{-1} \mathbf{e}_1}{\sqrt{\mathbf{e}_1^\top \Theta_{s_i, s_i}^{-1} \mathbf{e}_1}}, \quad (2.3)$$

where $s_i := \{j : (i, j) \in S\}$, $\Theta_{s_i, s_i}^{-1} := (\Theta_{s_i, s_i})^{-1}$ where Θ_{s_i, s_i} is the restriction of Θ to the set of indices s_i , and $\mathbf{e}_1 \in \mathbb{R}^{\#s_i \times 1}$ is the vector with the first entry equal to one and all other entries equal to zero. Using this formula, L can be computed in computational complexity $\mathcal{O}(\#S + (\max_{1 \leq i \leq N} \#s_i)^2)$ in space and $\mathcal{O}(\sum_{i=1}^N (\#s_i)^3)$ in time.

Proof. See Section A.1 of the appendix. □

Compared to ordinary sparse Cholesky factorization (see Algorithm 4), the algorithm implied by Theorem 2.1 has the advantage of giving the *best* possible Cholesky factor (as measured by KL) for a given sparsity pattern. Furthermore, it is embarrassingly parallel — all evaluations of Equation (2.3) can be performed independently for different i . While the computational complexity is slightly worse than the one of in-place incomplete Cholesky factorization, we will show in Theorem 3.4 that for important choices of S , the time complexity can be reduced to $\mathcal{O}(\sum_{k=1}^N (\#s_k)^2)$, matching the computational complexity of incomplete Cholesky factorization.

The formula in Equation (2.3) can be shown to be equivalent to the formula that has been used to compute the Vecchia approximation (Vecchia, 1988) in spatial statistics, without explicit awareness of the KL-optimality of the resulting L . In the literature on factorized sparse approximate inverses, the above formula was derived for minimizers of $\|\text{Id} - L \text{chol}(\Theta)\|_{\text{FRO}}$ subject to the constraints $L \in \mathcal{S}$ and $\text{diag}(L\Theta L^\top) = 1$ (Kolotilina and Yeregin, 1993), and for minimizers of the Kaporin condition number $(\text{trace}(\Theta LL^\top)/N)^N / \det(\Theta(LL^\top))$ subject to the constraint $L \in \mathcal{S}$ (Kaporin, 1990). The KL-divergence, as opposed to $\|\text{Id} - L \text{chol}(\Theta)\|_{\text{FRO}}$, strongly penalizes zero eigenvalues of ΘLL^\top , which explains the observation of Eremin et al. (1998) that adding the constraint $\text{diag}(L\Theta L^\top) = 1$ tends to improve the spectral condition number of the resulting preconditioner, despite increasing the size of the fidelity term $\|\text{Id} - L \text{chol}(\Theta)\|_{\text{FRO}}$. Marzouk et al. (2017) showed that the embarrassingly parallel nature of KL-minimization is even preserved when replacing the Cholesky factors with nonlinear transport maps with Knothe-Rosenblatt structure. As part of ongoing work on the sample complexity of the estimation of transport maps, Baptista et al. (2020) discovered representations very similar to Equation (2.3), independently of the present work.

Based on the results above, we propose the following procedure to approximate a large positive-definite matrix Θ :

1. Order the degrees of freedom (i.e., rows and columns of Θ) according to some ordering \prec .
2. Pick a sparsity set $S \subset I \times I$.
3. Use Formula (2.3) to compute the lower-triangular matrix L with nonzero entries contained in S that minimizes $D_{\text{KL}}(\mathcal{N}(0, \Theta) \parallel \mathcal{N}(0, (LL^\top)^{-1}))$.

In the next section, we will describe how to implement all three steps of this procedure in the more concrete setting of positive-definite matrices obtained from the evaluation of a finitely smooth covariance function at pairs of points in \mathbb{R}^d .

3 Ordering and sparsity pattern motivated by the screening effect

The quality of the approximation given by Equation (2.2) depends on the ordering of the variables and the sparsity pattern S . For kernel matrices arising from finitely smooth Gaussian processes we propose specific orderings and sparsity patterns, which can be constructed in near-linear computational complexity and which lead to good approximations for many Θ of practical interest.

3.1 The reverse-maximin ordering and sparsity pattern

Assume that G is the covariance function of a Gaussian process that is conditioned to be zero on (the possibly empty set) $\partial\Omega$, and the kernel matrix $\Theta \in \mathbb{R}^{I \times I}$ is obtained as $\Theta_{ij} := G(x_i, x_j)$ for a set of locations $\{x_i\}_{i \in I} \subset \Omega$.

The *reverse maximum-minimum distance (reverse-maximin) ordering* (Guinness, 2018; Schäfer

Algorithm 1: Without aggregation	Algorithm 2: With aggregation
Data: $G, \{x_i\}_{i \in I}, \prec, S_{\prec, l, \rho}$ Result: $L \in \mathbb{R}^{N \times N}$ lower triangular in \prec	Data: $G, \{x_i\}_{i \in I}, \prec, S_{\prec, l, \rho, \lambda}$ Result: $L \in \mathbb{R}^{N \times N}$ lower triangular in \prec
for $k \in I$ do for $i, j \in s_k$ do $(\Theta_{s_k, s_k})_{ij} \leftarrow G(x_i, x_j);$ $L_{s_k, k} \leftarrow \Theta_{s_k, s_k}^{-1} \mathbf{e}_k;$ $L_{s_k, k} \leftarrow L_{s_k, k} / L_{k, k};$ return $L;$	for $\tilde{k} \in \tilde{I}$ do for $i, j \in s_{\tilde{k}}$ do $(\Theta_{s_{\tilde{k}}, s_{\tilde{k}}})_{ij} \leftarrow G(x_i, x_j);$ $U \leftarrow P^\uparrow \text{chol}(P^\uparrow \Theta_{s_{\tilde{k}}, s_{\tilde{k}}} P^\uparrow) P^\uparrow;$ for $k \rightsquigarrow \tilde{k}$ do $L_{s_k, k} \leftarrow U^{-\top} \mathbf{e}_k;$ return $L;$

Figure 1: KL-minimization with and without using aggregation. For notational convenience, all matrices are assumed to have row- and column ordering according to \prec . P^\uparrow denotes the order-reversing permutation matrix, and $(\mathbf{e}_k)_l := \delta_{kl}$.

et al., 2017) of $\{x_i\}_{i \in I}$ is achieved by selecting the last index as

$$i_N := \operatorname{argmax}_{i \in I} \operatorname{dist}(x_i, \partial\Omega)$$

(or arbitrarily for $\partial\Omega = \emptyset$), and then choosing sequentially for $k = N - 1, N - 2, \dots, 1$ the index that is furthest away from $\partial\Omega$ and those indices that were already picked:

$$i_k := \operatorname{argmax}_{i \in I \setminus \{i_{k+1}, \dots, i_N\}} \operatorname{dist}(x_i, \{x_{i_{k+1}}, \dots, x_{i_N}\} \cup \partial\Omega).$$

Write $l_{i_k} = \operatorname{dist}(x_{i_k}, \{x_{i_{k+1}}, \dots, x_{i_N}\} \cup \partial\Omega)$, and write $i \prec j$ if i precedes j in the reverse-maximin ordering. We collect the $\{l_i\}_{i \in I}$ into a vector denoted by l .

For a tuning parameter $\rho \in \mathbb{R}^+$, we select the sparsity set $S_{\prec, l, \rho} \subset I \times I$ as

$$S_{\prec, l, \rho} := \{(i, j) : i \succeq j, \operatorname{dist}(x_i, x_j) \leq \rho l_j\}.$$

By a minor adaptation of Schäfer et al. (2017, Alg. 3), the reverse-maximin ordering and sparsity pattern can be constructed using Algorithm 7 (see Appendix B) in computational complexity $\mathcal{O}(N \log^2(N) \rho^{\tilde{d}})$ in time and $\mathcal{O}(N \rho^{\tilde{d}})$ in space, where $\tilde{d} \leq d$ is the intrinsic dimension of the dataset, as will be defined in Condition 3.2. The inverse Cholesky factors L can then be computed using Equation (2.3), as in Algorithm 1.

3.2 Aggregated sparsity pattern

It was already observed by Ferronato et al. (2015) in the context of sparse approximate inverses, and by Guinness (2018) in the context of the Vecchia approximation, that a suitable grouping of the degrees of freedom makes it possible to *reuse* Cholesky factorizations of the matrices Θ_{s_i, s_i} in Equation (2.3) to update multiple columns at once. Both of these prior works propose heuristics based on the sparsity graph of L and show empirically that they lead to improved performance. In contrast, we propose a grouping procedure based on geometric information and prove rigorously

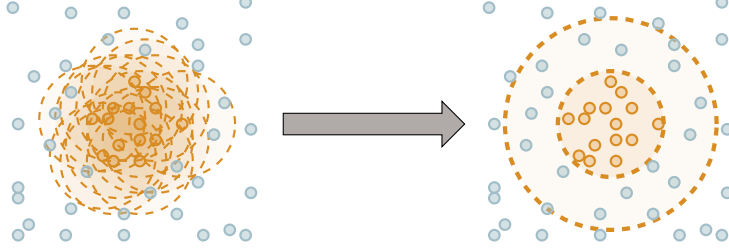


Figure 2: The left figure illustrates the original pattern $S_{\prec,l,\rho}$. For each orange point, we need to keep track of its interactions with all points within a circle of radius $\approx \rho$. In the right figure, the points have been collected into a supernode, which can be represented by a list of *parents* (the orange points within an inner sphere of radius $\approx \rho$) and *children* (all points within a radius $\approx 2\rho$).

that it allows us to reach the best asymptotic complexity in the literature, in a more concrete setting.

Assume that we have already computed the reverse-maximin ordering \prec and sparsity pattern $S_{\prec,l,\rho}$ and that we have access to the l_i as defined above. We will now aggregate the points into groups called *supernodes*, consisting of points that are close in both location and ordering. To do so, we pick at each step the first (w.r.t. \prec) index $i \in I$ that has not been aggregated into a supernode yet and then we aggregate into a common supernode the indices in $\{j : (i, j) \in S_{\prec,l,\rho}, l_j \leq \lambda l_i\}$ for some $\lambda > 1$ ($\lambda \approx 1.5$ is typically a good choice) that have not been aggregated yet. We proceed with this procedure until every node has been aggregated into a supernode. We write \tilde{I} for the set of all supernodes; for $i \in I, \tilde{i} \in \tilde{I}$, we write $i \rightsquigarrow \tilde{i}$ if \tilde{i} is the supernode to which i has been aggregated. We furthermore define $s_{\tilde{i}} := \{j : \exists i \rightsquigarrow \tilde{i}, j \in s_i\}$ and introduce the aggregated sparsity pattern $\tilde{S}_{\prec,l,\rho,\lambda} := \bigcup_{k \rightsquigarrow \tilde{k}} \{(i, k) : k \preceq i \in s_{\tilde{k}}\}$. This sparsity pattern, while larger than $S_{\prec,l,\rho}$, can be represented efficiently by keeping track of the set of *parents* (the $k \in I$ such that $k \rightsquigarrow \tilde{k}$) and *children* (the $i \in s_{\tilde{k}}$) of each supernode, rather than the individual entries (see Figure 2 for an illustration). For well-behaved (cf. Theorem 3.4) sets of points, we obtain $\mathcal{O}(N\rho^{-d})$ supernodes, each with $\mathcal{O}(\rho^d)$ parents and children, thus improving the cost of storing the sparsity pattern from $\mathcal{O}(N\rho^d)$ to $\mathcal{O}(N)$.

While the above aggregation procedure can be performed efficiently once \prec and $S_{\prec,l,\rho}$ are computed, it is possible to directly compute \prec and an outer approximation $\tilde{S}_{\prec,l,\rho,\lambda} \supset \tilde{S}_{\prec,l,\rho,\lambda}$ in computational complexity $\mathcal{O}(N)$ in space and $\mathcal{O}(N \log(N))$ in time. $\tilde{S}_{\prec,l,\rho,\lambda}$ can either be used directly, or it can be used to compute $\tilde{S}_{\prec,l,\rho,\lambda}$ in $\mathcal{O}(N)$ in space and $\mathcal{O}(N \log(N)\rho^d)$ in time, using a simple and embarrassingly parallel algorithm. Details are given in Appendix B.

In addition to reducing the memory cost, the aggregated ordering and sparsity pattern allows us to compute the Cholesky factors (in reverse ordering) $\Theta_{s_{\tilde{k}},s_{\tilde{k}}} = UU^\top$ once for each supernode and then use it to compute the $L_{s_k,k}$ for all $k \rightsquigarrow \tilde{k}$ as in Algorithm 2 (see Figure 3 for an illustration). As we show in the next section, this allows us to reduce the computational complexity from $\mathcal{O}(N\rho^{3d})$ to $\mathcal{O}(N\rho^{2d})$ for sufficiently well-behaved sets of points.

3.3 Theoretical guarantees

Our theoretical results apply to more general orderings, called reverse r -maximin orderings, which for $r \in (0, 1]$ have the following property.

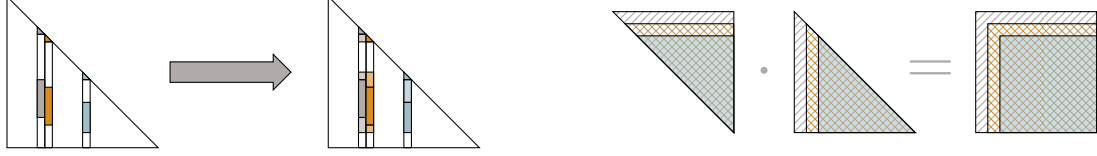


Figure 3: (Left:) By adding a few nonzero entries to the sparsity pattern, the sparsity patterns of columns in $s_{\tilde{k}}$ become subsets of one another. (Right:) Therefore, the matrices $\{\Theta_{s_k, s_k}\}_{k \rightsquigarrow \tilde{k}}$, which need to be inverted to compute the columns in \tilde{k} , become submatrices of one another. Thus, submatrices of the Cholesky factorization of the Θ_{s_k, s_k} corresponding to the first column can be used as Cholesky factors for the later columns in \tilde{k} .

Definition 3.1. An elimination ordering \prec is called reverse r -maximin with length scales $\{l_i\}_{i \in I}$ if for every $j \in I$ we have

$$l_j := \min_{i \succ j} \text{dist}(x_j, \{x_i\} \cup \partial\Omega) \geq r \max_{j \succ k} \min_{i \succ j} \text{dist}(x_k, \{x_i\} \cup \partial\Omega).$$

We note that the reverse maximin ordering from Section 3.1 is a reverse 1-maximin ordering; reverse r -maximin orderings with $r < 1$ can be computed in computational complexity $\mathcal{O}(N \log(N))$ (see Appendix B). We define the sparsity patterns $S_{\prec, l, \rho}$ and $\tilde{S}_{\prec, l, \rho, \lambda}$ analogously to the case of the reverse maximin ordering, and we will write L^ρ for the incomplete Cholesky factors of Θ^{-1} computed using Equation 2.3 based on the sparsity pattern $S_{\prec, l, \rho}$ or $\tilde{S}_{\prec, l, \rho, \lambda}$.

3.3.1 Computational complexity

One advantage of our method is that the computational complexity depends only on the *intrinsic* dimension of the dataset, not on the dimension of the ambient space.

Condition 3.2 (Intrinsic dimension). We say that $\{x_i\}_{i \in I} \subset \mathbb{R}^d$ has intrinsic dimension \tilde{d} if there exists a constant $C_{\tilde{d}}$, independent of N , such that for all $r, R > 0$, $x \in \mathbb{R}^d$, we have

$$\max \{|A| : i, j \in A \Rightarrow \text{dist}(x_i, x), \text{dist}(x_j, x) \leq R, \text{dist}(x_i, x_j) \geq r\} \leq C_{\tilde{d}} (R/r)^{\tilde{d}}$$

We also make a mild technical assumption requiring that most of the points belong to the finer scales of the ordering:

Condition 3.3 (Regular refinement). We say that $\{x_i\}_{i \in I} \subset \mathbb{R}^d$ fulfills the regular refinement condition for λ and l with constant $C_{\lambda, l}$, if

$$\sum_{k=\lfloor \log(l_1)/\log(\lambda) \rfloor}^{\infty} \#\{i : \lambda^k \leq l_i\} \leq C_{\lambda, l} N$$

This condition excludes pathological cases like $x_i = 2^{-i}$ for which each scale contains the same number of points.

Analogously to the results of Schäfer et al. (2017), we obtain the following computational complexity:

Theorem 3.4. *Under Condition 3.2 with $C_{\tilde{d}}$ and \tilde{d} , using an r -reverse maximin ordering \prec and $S_{\prec,l,\rho}$, Algorithm 1 computes L^ρ in complexity $CN\rho^{\tilde{d}}$ in space and $CN\rho^{3\tilde{d}}$ in time. If we assume in addition that $\{x_i\}_{i \in I}$ fulfills Condition 3.3 for λ and l with constant $C_{\lambda,l}$, then, using $\tilde{S}_{\prec,l,\rho,\lambda}$ or $\bar{S}_{\prec,l,\rho,\lambda}$, Algorithm 2 computes L^ρ in complexity $CN\rho^{\tilde{d}}$ in space and $C_{\lambda,l}CN\rho^{2\tilde{d}}$ in time. Here, the constant C depends only on $C_{\tilde{d}}$, \tilde{d} , r , λ , and the maximal cost of evaluating a single entry of Θ , but not on N or d .*

Proof. See Section C of the appendix. □

3.3.2 Approximation error

We derive rigorous bounds on the approximation error from results on the localisation of stiffness matrices of *gamblets* (a class of operator-adapted wavelets) proved by Owhadi and Scovel (2017, 2019), and their interpretation as Cholesky factors introduced by Schäfer et al. (2017). Thus, the bounds hold in the setting of the above references. We assume for the purpose of this section that Ω is a bounded domain of \mathbb{R}^d with Lipschitz boundary, and for an integer $s > d/2$, we write $H_0^s(\Omega)$ for usual Sobolev the space of functions with zero Dirichlet boundary values and order s derivatives in L^2 , and $H_0^{-s}(\Omega)$ for its dual. Let the operator

$$\mathcal{L} : H_0^s(\Omega) \mapsto H^{-s}(\Omega),$$

be linear, symmetric ($\int u\mathcal{L}v = \int v\mathcal{L}u$), positive ($\int u\mathcal{L}u \geq 0$), bijective, bounded (write $\|\mathcal{L}\| := \sup_u \|\mathcal{L}u\|_{H^{-s}(\Omega)} / \|u\|_{H_0^s(\Omega)}$ for its operator norm), and local in the sense that $\int u\mathcal{L}v dx = 0$, for all $u, v \in H_0^s(\Omega)$ with disjoint support. By the Sobolev embedding theorem, we have $H_0^s(\Omega) \subset C_0(\Omega)$ and hence $\{\delta_x\}_{x \in \Omega} \subset H^{-s}(\Omega)$. We then define G as the Green's function of \mathcal{L} ,

$$G(x_1, x_2) := \int \delta_{x_1} \mathcal{L}^{-1} \delta_{x_2} dx.$$

A simple example when $d = 1$ and $\Omega = (0, 1)$, is $\mathcal{L} = -\Delta$, and $G(x, y) = \mathbb{1}_{x < y} \frac{1-y}{1-x} + \mathbb{1}_{y \leq x} \frac{y}{x}$. Let us define the following measure of *homogeneity* of the distribution of the $\{x_i\}_{i \in I}$,

$$\delta := \frac{\min_{i,j \in I} \text{dist}(\{i\}, \{j\} \cup \partial\Omega)}{\max_{x \in \Omega} \text{dist}(x, \{x_i\}_{i \in I} \cup \partial\Omega)}.$$

Using the above definitions, we can rigorously quantify the increase in approximation accuracy as ρ increases.

Theorem 3.5. *Using an r -maximin ordering \prec and sparsity patterns $S_{\prec,l,\rho}$ or $\tilde{S}_{\prec,l,\rho,\lambda}$, there exists a constant C depending only on d , Ω , r , λ , s , $\|\mathcal{L}\|$, $\|\mathcal{L}^{-1}\|$, and δ , such that for $\rho \geq C \log(N/\epsilon)$, we have*

$$D_{\text{KL}}(\Theta \parallel (L^\rho L^{\rho,\top})^{-1}) + \|\Theta - (L^\rho L^{\rho,\top})^{-1}\|_{\text{FRO}} \leq \epsilon$$

Thus, Algorithm 1 computes an ϵ -accurate approximation of Θ in computational complexity $CN \log^d(N/\epsilon)$ in space and $CN \log^{3d}(N/\epsilon)$ in time, from only $CN \log^d(N/\epsilon)$ entries of Θ . Similarly, Algorithm 2 computes an ϵ -accurate approximation of Θ in computational complexity $CN \log^d(N/\epsilon)$ in space and $CN \log^{2d}(N/\epsilon)$ in time, from only $CN \log^d(N/\epsilon)$ entries of Θ .

To the best of our knowledge, the above result is the best known complexity/accuracy trade-off for kernel matrices based on Green’s functions of elliptic boundary value problems. Some related but slower or less practically useful approaches were presented in Schäfer et al. (2017), who showed that the Cholesky factors of Θ (as opposed to those of Θ^{-1}) can be approximated in computational complexity $\mathcal{O}(N \log^2(N) \log^{2d}(N/\epsilon))$ in time and $\mathcal{O}(N \log(N) \log^d(N/\epsilon))$ in space using zero-fill-in incomplete Cholesky factorization (Algorithm 4) applied to Θ . Similarly, they showed that the Cholesky factors of Θ^{-1} can be approximated in computational complexity $\mathcal{O}(N \log^{2d}(N/\epsilon))$ in time and $\mathcal{O}(N \log^d(N/\epsilon))$ in space using zero-fill-in incomplete Cholesky factorization applied to Θ^{-1} . While they also observed that the near-sparsity of the Cholesky factors of Θ^{-1} implies that they can in principle be computed in computational complexity $\mathcal{O}(N \log^{2d}(N/\epsilon))$ from entries of Θ by a recursive algorithm (thus improving the complexity of inverting Θ), they did not provide an explicit algorithm for this purpose. Indeed, we have found that recursive algorithms based on truncation are unstable to the point of being useless in practice, when used to compute the Cholesky factors of Θ^{-1} from entries of Θ .

4 Extensions

We now present extensions of our method that improve its performance in practice. In Section 4.1, we show how to improve the approximation when Θ is replaced by $\Theta + R$, for R diagonal, as is frequently the case in statistical inference where R is the covariance matrix of additive, independent noise. In Section 4.2, we discuss memory savings and parallel computation for GP inference when we are only interested in computing the likelihood and the posterior mean and covariance, as opposed to, for example, sampling from $\mathcal{N}(0, \Theta)$ or computing products $v \mapsto \Theta v$. In Section 4.3, we show how including the prediction points can improve the computational complexity (Section 4.3.1) or accuracy (Section 4.3.2) of the posterior mean and covariance.

We note that it is not possible to combine the variant in Section 4.1 with that in Section 4.2, and that the combination of the variants in Section 4.1 and 4.3.2 might diminish accuracy gains from the latter. Furthermore, while Section 4.2 can be combined with Section 4.3.1 to compute the posterior mean, this combination cannot be used to compute the full posterior covariance matrix.

4.1 Additive noise

Assume that a diagonal noise term is added to Θ , so that $\Sigma = \Theta + R$, where R is diagonal. Extending the Vecchia approximation to this setting has been a major open problem in spatial statistics (Datta et al., 2016; Katzfuss and Guinness, 2019; Katzfuss et al., 2018). Applying our approximation to Σ directly would not work well, because the noise term attenuates the exponential decay. Instead, given the approximation $\hat{\Theta}^{-1} = LL^\top$ obtained using our method, we can write, following Schäfer et al. (2017):

$$\Sigma \approx \hat{\Theta} + R = \hat{\Theta}(R^{-1} + \hat{\Theta}^{-1})R.$$

Applying an incomplete Cholesky factorization with zero fill-in (Algorithm 4) to $R^{-1} + \hat{\Theta}^{-1} \approx \tilde{L}\tilde{L}^\top$, we have

$$\Sigma \approx (LL^\top)^{-1}\tilde{L}\tilde{L}^\top R.$$

The resulting procedure, given in Algorithm 3, has asymptotic complexity $\mathcal{O}(N\rho^{2d})$, because every column of the triangular factors has at most $\mathcal{O}(\rho^d)$ entries.

<p>Algorithm 3: Including independent noise with covariance matrix R</p> <p>Data: $G, \{x_i\}_{i \in I}, \rho, (\lambda,)$ and R</p> <p>Result: $L, \tilde{L} \in \mathbb{R}^{N \times N}$ l. triangular in \prec</p> <p>Compute \prec and $S \leftarrow S_{\prec, l, \rho}(S \leftarrow S_{\prec, l, \rho, \lambda})$; Compute L using Algorithm 1(2);</p> <p>for $(i, j) \in S$ do</p> <p style="padding-left: 2em;">⌊ $A_{ij} \leftarrow \langle L_{i,:}, L_{j,:} \rangle$;</p> <p>$A \leftarrow A + R$;</p> <p>$\tilde{L} \leftarrow \text{ichol}(A, S)$;</p> <p>return L, \tilde{L};</p>	<p>Algorithm 4: Zero fill-in incomplete Cholesky factorization ($\text{ichol}(A, S)$)</p> <hr/> <p>Data: $A \in \mathbb{R}^{N \times N}, S$</p> <p>Result: $L \in \mathbb{R}^{N \times N}$ l. triangular in \prec</p> <p>$L \leftarrow (0, \dots, 0)(0, \dots, 0)^\top$;</p> <p>for $j \in \{1, \dots, N\}$ do</p> <p style="padding-left: 2em;">for $i \in \{j, \dots, N\} : (i, j) \in S$ do</p> <p style="padding-left: 4em;">⌊ $L_{ij} \leftarrow A_{ij} - \langle L_{i,1:(j-1)}, L_{j,1:(j-1)} \rangle$;</p> <p style="padding-left: 4em;">⌊ $L_{:i} \leftarrow A_{:i} / \sqrt{A_{ii}}$;</p> <p>return L;</p>
---	--

Figure 4: Algorithms for approximating covariance matrices with added independent noise $\Theta + R$ (left), using the zero fill-in incomplete Cholesky factorization (right). See Section 4.1.

Following the intuition that Θ^{-1} is *essentially* an elliptic partial differential operator, $\Theta^{-1} + R^{-1}$ is *essentially* a partial differential operator with an added zero-order term, and its Cholesky factors can thus be expected to satisfy an exponential decay property just as those of Θ^{-1} . Indeed, as observed by Schäfer et al. (2017, Fig. 2.3), the exponential decay of the Cholesky factors of $R^{-1} + \Theta^{-1}$ is as strong as for Θ^{-1} , even for large R . We suspect that this could be proved rigorously by adapting the proof of exponential decay in Owhadi and Scovel (2019) to the discrete setting. We note that while independent noise is most commonly used, the above argument leads to an efficient algorithm whenever R^{-1} is approximately given by an elliptic PDE (possibly of order zero).

For small ρ , the additional error introduced by the incomplete Cholesky factorization can harm accuracy, which is why we recommend using the conjugate gradient algorithm (CG) to invert $(R^{-1} + \hat{\Theta}^{-1})$ using \tilde{L} as a preconditioner. In our experience, CG converges to single precision in a small number of iterations (~ 10).

Alternatively, higher accuracy can be achieved by using the sparsity pattern of LL^\top (as opposed to that of L) to compute the incomplete Cholesky factorization of A in Algorithm 3; in fact, in our numerical experiments in Section 5.2, this approach was as accurate as using the exact Cholesky factorization of A over a wide range of ρ values and noise levels. The resulting algorithm still requires $\mathcal{O}(N\rho^{2d})$ time, albeit with a larger constant. This is because for an entry (i, j) to be part of the sparsity pattern of LL^\top , there needs to exist a k such that both (i, k) and (j, k) are part of the sparsity pattern of L . By the triangle inequality, this implies that (i, j) is contained in the sparsity pattern of L obtained by doubling ρ . In conclusion, we believe that the above modifications allow us to compute an ϵ -accurate factorization in $\mathcal{O}(N \log^{2d}(N/\epsilon))$ time and $\mathcal{O}(N \log^d(N/\epsilon))$ space, just as in the noiseless case.

4.2 GP regression in $\mathcal{O}(N + \rho^{2\tilde{d}})$ space complexity

When deploying direct methods for approximate inversion of kernel matrices, a major difficulty is the superlinear memory cost that they incur. This in particular poses difficulties in a distributed setting or on graphics processing units. In the following, $I = I_{\text{Tr}}$ denotes the indices of the training data, while I_{Pr} denotes those of the points where we want to predict. Accordingly, we

use the subscripts Tr and Pr to refer to the training and prediction variables, respectively. For GP regression with training data y , training covariance matrix $\Theta = \Theta_{\text{Tr},\text{Tr}}$, training-prediction covariance $\Theta_{\text{Tr},\text{Pr}}$, and the prediction covariance matrix $\Theta_{\text{Pr},\text{Pr}}$, we are mainly interested in the following computational operations:

- Computation of the log-likelihood proportional to $y^\top \Theta^{-1} y + \log \det \Theta + N \log(2\pi)$
- Computation of the posterior mean $y^\top \Theta^{-1} \Theta_{\text{Tr},\text{Pr}}$
- Computation of the posterior covariance $\Theta_{\text{Pr},\text{Pr}} - \Theta_{\text{Pr},\text{Tr}} \Theta^{-1} \Theta_{\text{Tr},\text{Pr}}$

In order to compute the log-likelihood, we need to compute the matrix-vector product $L^{\rho,\top} y$, as well as the diagonal entries of L^ρ . This can be done by computing the columns $L_{:,k}$ of L individually using Equation 2.3 and setting $(L^{\rho,\top} y)_k = (L_{:,k}^\rho)^\top y$, $L_{kk}^\rho = (L_{:,k}^\rho)_k$, without ever forming the matrix L^ρ . Similarly, in order to compute the posterior mean, we only need to compute $\Theta^{-1} y = L^{\rho,\top} L^\rho y$, which only requires us to compute each column of L^ρ twice, without ever forming the entire matrix. In order to compute the posterior covariance, we need to compute the matrix-matrix product $L^{\rho,\top} \Theta_{\text{Tr},\text{Pr}}$, which again can be performed by computing each column of L^ρ once without ever forming the entire matrix L^ρ . However, it does require us to know beforehand at which points we want to make predictions. The submatrices Θ_{s_i, s_i} for all i belonging to the supernode \tilde{k} (i.e., $i \rightsquigarrow \tilde{k}$) can be formed from a list of the elements of \tilde{s}_k . Thus, the overall memory complexity of the resulting algorithm is $\mathcal{O}(\sum_{k \in \tilde{I}} \#\tilde{s}_k) = \mathcal{O}(N + \rho^{2\tilde{d}})$. The above described procedure is implemented in Algorithms 5 and 6 in Section A.3. In a distributed setting with workers W_1, W_2, \dots , this requires communicating only $\mathcal{O}(\#\tilde{s}_k)$ floating-point numbers to worker W_k , which then performs $\mathcal{O}((\#\tilde{s}_k)^3)$ floating-point operations; a naive implementation would require the communication of $\mathcal{O}((\#\tilde{s})^2)$ floating-point numbers to perform the same number of floating-point operations.

4.3 Including the prediction points

In the setting of Theorem 3.5, our method can be applied to accurately approximate the matrix Θ in near-linear cost. The training covariance matrix can then be replaced by the resulting approximation for all downstream applications (e.g., as in Section 4.2). Its application to the approximation of the joint covariance matrix of training and prediction variables improves (1) stability and accuracy compared to computing the KL-optimal approximation of the training covariance alone, (2) computational complexity by circumventing the computation of most of the $N_{\text{Tr}} N_{\text{Pr}}$ entries of the off-diagonal part $\Theta_{\text{Tr},\text{Pr}}$ of the covariance matrix. We can add the prediction points before or after the training points in the elimination ordering.

4.3.1 Ordering the prediction points first, for rapid interpolation

The computation of the mixed covariance matrix $\Theta_{\text{Pr},\text{Tr}}$ can be prohibitively expensive when interpolating with a large number of prediction points. This situation is common in spatial statistics when estimating a stochastic field throughout a large domain. In this regime, we propose to order the $\{x_i\}_{i \in I}$ by first computing the reverse maximin ordering \prec_{Tr} of only the training points as described in Section 3.1 using the original Ω , writing l_{Tr} for the corresponding length scales. We then compute the reverse maximin ordering \prec_{Pr} of the prediction points using the modified $\tilde{\Omega} := \Omega \cup \{x_i\}_{i \in I_{\text{Tr}}}$, obtaining the length scales l_{Pr} . Since $\tilde{\Omega}$ contains $\{x_i\}_{i \in I_{\text{Tr}}}$, when computing the ordering of the prediction points, prediction points close to the training set will tend to have a smaller length-scale than in the naive application of the algorithm and thus the resulting sparsity pattern will have fewer nonzero entries. We then order the prediction points before the training

points and compute $S_{(\prec_{\text{Pr}}, \prec_{\text{Tr}}), (l_{\text{Pr}}, l_{\text{Tr}}), \rho}$ or $S_{(\prec_{\text{Pr}}, \prec_{\text{Tr}}), (l_{\text{Pr}}, l_{\text{Tr}}), \rho, \lambda}$ following the same procedure as in Sections 3.1 and 3.2, respectively. The distance of each point in the prediction set to the training set can be computed in near-linear complexity using, for example, a minor variation of Schäfer et al. (2017, Alg. 3). Writing L for the resulting Cholesky factor of the joint precision matrix, we can approximate $\Theta_{\text{Pr}, \text{Pr}} \approx L_{\text{Pr}, \text{Pr}}^{-\top} L_{\text{Pr}, \text{Pr}}^{-1}$ and $\Theta_{\text{Pr}, \text{Tr}} \approx L_{\text{Pr}, \text{Pr}}^{-\top} L_{\text{Tr}, \text{Pr}}^{\top}$ based on submatrices of L . See Section D.1 and Algorithm 11 for additional details. We note that the idea of ordering the prediction points first (last, in their notation) has already been proposed by Katzfuss et al. (2018) in the context of the Vecchia approximation, although without providing an explicit algorithm. If one does not use the method in Section 4.1 to treat additive noise, then the method described in this section amounts to making each prediction using only $\mathcal{O}(\rho^d)$ nearby datapoints. In the extreme case where we only have a single prediction point, this means that we are only using $\mathcal{O}(\rho^d)$ training values for prediction. On the one hand, this can lead to improved robustness of the resulting estimator, but on the other hand it can lead to some training data being missed entirely.

4.3.2 Ordering the prediction points last, for improved robustness

If we want to use the improved stability of including the prediction points, maintain near-linear complexity, and use all N_{Tr} training values for the prediction of even a single point, we have to include the prediction points *after* the training points in the elimination ordering. Naively, this would lead to a computational complexity of $\mathcal{O}(N(\rho^d + N_{\text{Pr}})^2)$, which might be prohibitive for large values of N_{Pr} . If it is enough to compute the posterior covariance only among m_{Pr} small *batches* of up to n_{Pr} predictions each (often, it makes sense to choose $n_{\text{Pr}} = 1$), we can avoid this increase of complexity by performing prediction on groups of only n_{Pr} at once, with the computation for each batch only having computational complexity $\mathcal{O}(N(\rho^d + n_{\text{Pr}})^2)$. A naive implementation would still require us to perform this procedure m_{Pr} times, eliminating any gains due to the batched procedure. However, careful use of the Sherman-Morrison-Woodbury matrix identity allows to reuse the biggest part of the computation for each of the batches, thus reducing the computational cost for prediction and computation of the covariance matrix to only $\mathcal{O}(N((\rho^d + n_{\text{Pr}})^2 + (\rho^d + n_{\text{Pr}})m_{\text{Pr}}))$. This procedure is detailed in Section D.2 and summarized in Algorithm 13.

5 Applications and numerical results

We conclude with numerical experiments studying the practical performance of our method. The Julia code can be found under https://github.com/f-t-s/cholesky_by_KL_minimization.

5.1 Gaussian-process regression and aggregation

We begin our numerical experiments with two dimensional ($d = 2$) synthetic data. We use the FFT (Gutjahr et al., 1997)[<https://github.com/JuliaEarth/SpectralGaussianSimulation.jl>] to create 10^3 samples of a Gaussian process with exponential covariance function at $N = 10^6$ locations on a grid in $\Omega = [0, 1]^2$. From these, we select $N_{\text{Pr}} = 2 * 10^4$ prediction points, and use the remaining points as training data. As illustrated in Figure 5 (left panel), half of the prediction points form two elliptic regions devoid of any training points (called *region*), while the remaining prediction points are interspersed among the training points (called *scattered*). We then use the "prediction points first" approach of Section 4.3.1 and the aggregated sparsity pattern $\tilde{S}_{\prec, l, \rho, \lambda}$ of Section 3.2 with $\lambda \in \{1.0, 1.3\}$, to compute the posterior distributions at the prediction points from the values

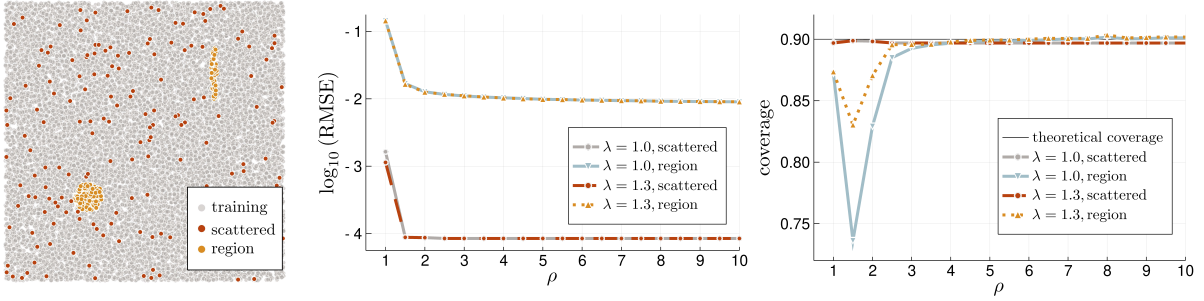


Figure 5: Accuracy of our approximation with and without aggregation for a Gaussian process with exponential covariance on a grid of size $N = 10^6$ on the unit square. (Left:) Randomly sampled 2 percent of the training and prediction points. (Middle:) RMSE, averaged over prediction points and 1,000 realizations. (Right:) Empirical coverage of 90% prediction intervals computed from the posterior covariance. We believe that the small discrepancy between the empirical and nominal coverage for large ρ is due to the approximation error incurred by the FFT sampling on a finite domain.

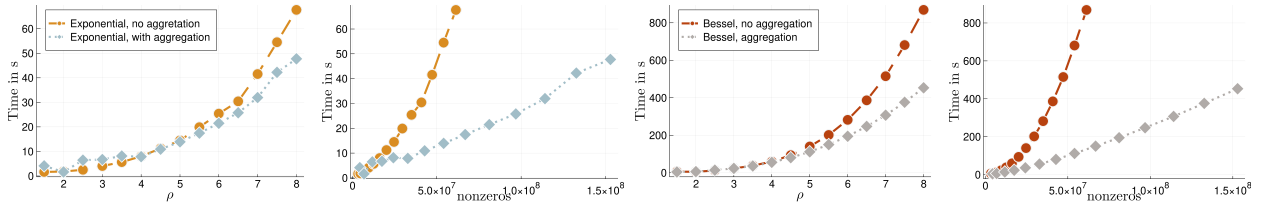


Figure 6: Time for computing the factor L with or without aggregation ($N = 10^6$), as a function of ρ and of the number of nonzero entries. For the first two panels, the Matérn covariance function was computed using a representation in terms of exponentials, while for the second two panels they were computed using (slower) Bessel function evaluations. Computations performed on an Intel®Core™i7-6400 CPU with 4.00GHz and 64 GB of RAM.

at the training points. In Figure 5, we report the RMSE of the posterior means, as well as the empirical coverage of the 90% posterior intervals, averaged over all 10^3 realizations, for a range of different ρ . Note that while the RMSE between the aggregated ($\lambda = 1.3$) and non-aggregated ($\lambda = 1.0$) is almost the same, the coverage converges significantly faster to the correct value. We further provide timing results for 10^6 training points uniformly distributed in $[0, 1]^2$ comparing the aggregated and non-aggregated version of the algorithm. As predicted by the theory, the aggregated variant scales better as we are increasing ρ . This holds true both when using Intel® `oneMKL Vector Mathematics` functions library to evaluate the exponential function, or when using `amos` to instead evaluate the modified Bessel function of the second kind. While the former is faster and emphasizes the improvement from $\mathcal{O}(N\rho^{3d})$ to $\mathcal{O}(N\rho^{2d})$ of complexity of computing the factorization, the latter can be used to evaluate Matérn kernels with arbitrary smoothness. Due to being slower, using Bessel functions highlights the improvement from needing $\mathcal{O}(N\rho^{2d})$ matrix evaluations without the aggregation to just $\mathcal{O}(N\rho^d)$. By plotting the the number of nonzeros used for the two approaches, we see that the aggregated version is faster to compute despite using many more entries of Θ than the non-aggregated version. Thus, aggregation is both faster and more

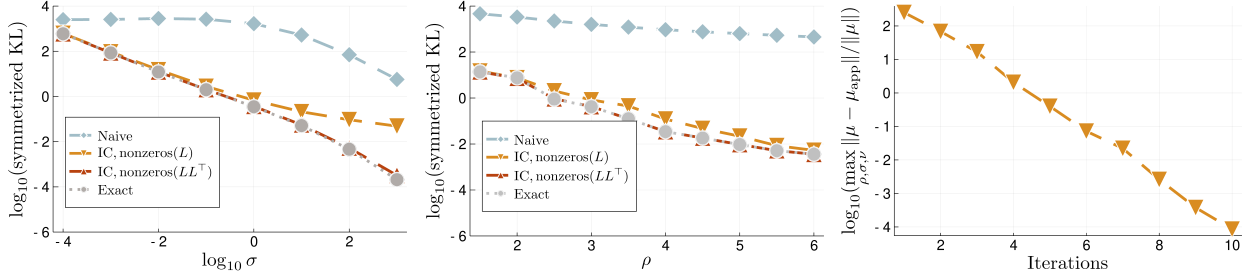


Figure 7: Comparison of the methods proposed in Section 7 for approximating $\Sigma = \Theta + R$, where Θ is based on a Matérn covariance with range parameter 0.5 and smoothness $\nu = 3/2$ at $N = 10^4$ uniformly sampled locations on the unit square, and $R = \sigma^2 I$ is additive noise. For each approximation, we compute the symmetrized KL divergence (the sum of the KL-divergences with either ordering of the two measures) to the true covariance. “Naive”: Directly apply Algorithm 2 to Σ . “Exact”: Apply Algorithm 2 to Θ , then compute \tilde{L} as the exact Cholesky factorization of $A := R^{-1} + \hat{\Theta}^{-1}$. “IC”: Apply Algorithm 2 to Θ , then compute \tilde{L} using incomplete Cholesky factorization of A on the sparsity pattern of either L or LL^\top . (Left:) Varying σ , fixed $\rho = 3.0$. (Middle:) Varying ρ , fixed $\sigma = 1.0$. (Right:) Maximal relative error (over the above $\sigma, \rho, \nu \in \{1/2, 3/2, 5/2\}$ and 10 random draws) of inverting A using up to 10 conjugate-gradient iterations, with IC, nonzeros(L) as preconditioner.

accurate for the same value of ρ , which is why we recommend using it over the non-aggregated variant.

5.2 Adding noise

We now experimentally verify the claim that the methods described in Section 4.1 enable accurate approximation in the presence of independent noise, while preserving the sparsity, and thus computational complexity, of our method. To this end, pick a set of $N = 10^4$ points uniformly at random in $\Omega = [0, 1]^2$, use a Matérn kernel with smoothness $\nu = 3/2$, and add I.I.D. noise with variance σ^2 . We use an aggregation parameter $\lambda = 1.5$. As shown in Figure 7, our approximation stays accurate over a wide range of values of both ρ and σ , even for the most frugal version of our method. The asymptotic complexity for both incomplete-Cholesky variants is $\mathcal{O}(N\rho^{2d})$, with the variant using the sparsity pattern of LL^\top being roughly equivalent to doubling ρ . Hence, to avoid additional memory overhead, we recommend using the sparsity pattern of L as a default choice; the accuracy of the resulting log-determinant of Σ should be sufficient for most settings, and the accuracy for solving systems of equations in Σ can easily be increased by adding a few iterations of conjugate gradient.

5.3 Including prediction points

We continue by studying the effects of including the prediction points in the approximation, as described in Sections 4.3.1 and 4.3.2. We compare not including the predictions points in the approximation with including them either before or after training points in the approximation. We compare the accuracy of the approximation of posterior mean and standard deviation over three different geometries and a range of different values for ρ . The results, displayed in Figure 5.3, show

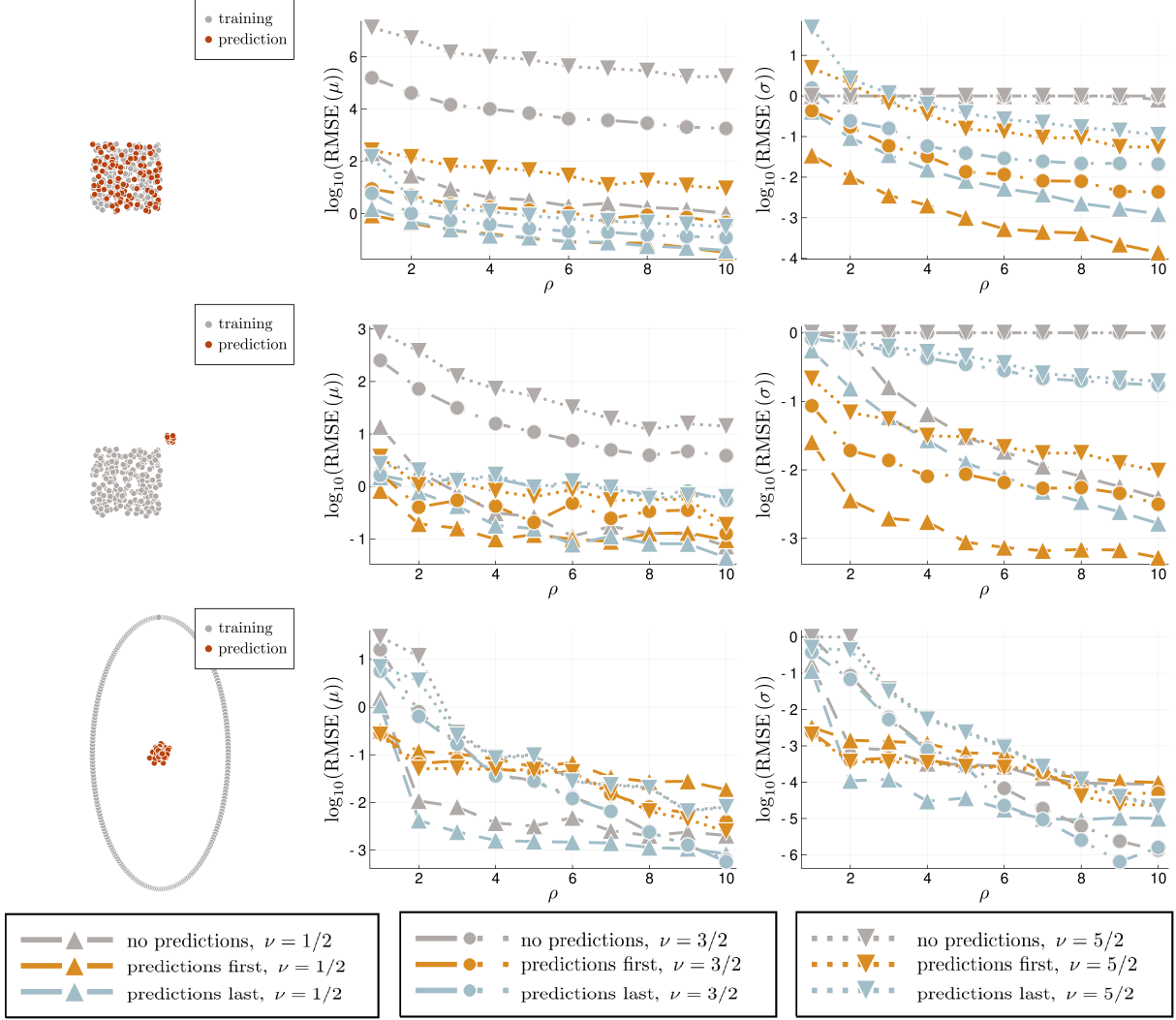


Figure 8: To analyze the effects of including the prediction points into the approximation, we consider three datasets. Each consists of $5 * 10^4$ training points and 10^2 test points, averaged over ten independent realizations of the Gaussian process. We use Matérn kernels with range parameter 0.5 and smoothness $\nu \in \{1/2, 3/2, 5/2\}$. We let ρ range from 1.0 to 10.0, without using aggregation. On the y -axis we plot the RMSE of the the posterior mean and standard deviation, scaled in each point by the reciprocal of the true posterior standard deviation.

that including the prediction points can increase the accuracy by multiple orders of magnitude. The performance difference between the two schemes for including prediction points varies over different geometries, degrees of regularity, and values of ρ . If the number of prediction points is comparable, the only way to avoid quadratic scaling in the number of points is to order the prediction points first, making this approach the method of choice. If we only have few prediction points, ordering the prediction variables last can improve the accuracy for low orders of smoothness, especially in settings in which only a small part of the training data is used in the prediction-variables-first approach (e.g., second row in Figure 5.3).

5.4 Single-layer boundary element methods

We now provide an application to boundary element methods. For a domain $\Omega \in \mathbb{R}^d$ with boundary $\partial\Omega$, let us assume that we want to solve the Dirichlet boundary value problem

$$\begin{aligned} -\Delta u(x) &= 0, & \forall x \in \Omega \\ u(x) &= g(x), & \forall x \in \partial\Omega. \end{aligned}$$

For $d = 3$, the Green's function of the Laplace operator is given by the gravitational / electrostatic potential

$$G_{\mathbb{R}^3}(x, y) = \frac{1}{4\pi|x - y|}.$$

Under mild regularity assumptions one can verify that

$$u = \int_{x \in \partial\Omega} G_{\mathbb{R}^3}(x, \cdot) h(x) dx, \quad \text{for } h \text{ the solution of } \quad g = \int_{x \in \partial\Omega} G_{\mathbb{R}^3}(x, \cdot) h(x) dx.$$

Let us choose finite dimensional basis functions $\{\phi_i\}_{i \in I_{Pr}}$ in the interior of Ω and $\{\phi_i\}_{i \in I_{Tr}}$ on the boundary of Ω . We form the symmetric matrix $\Theta \in \mathbb{R}^{(I_{Tr} \cup I_{Pr}) \times (I_{Tr} \cup I_{Pr})}$ as

$$\Theta_{ij} := \int_{x \in \mathcal{D}_i} \int_{y \in \mathcal{D}_j} \phi_i(x) G_{\mathbb{R}^3}(x, y) \phi_j(y) dy dx, \quad \text{where } \mathcal{D}_p = \begin{cases} \partial\Omega, & \text{for } p \in I_{Tr} \\ \Omega, & \text{for } p \in I_{Pr} \end{cases}$$

and denote as $\Theta_{Tr, Tr}$, $\Theta_{Tr, Pr}$, $\Theta_{Pr, Tr}$, $\Theta_{Pr, Pr}$ its restrictions to the rows and columns indexed by I_{Tr} or I_{Pr} . Defining

$$\vec{g}_i := \int_{x \in \partial\Omega} \phi_i(x) g(x) dx, \quad \forall i \in I_{Tr} \quad \text{and} \quad \vec{u}_i := \int_{x \in \partial\Omega} \phi_i(x) u(x) dx, \quad \forall i \in I_{Pr},$$

we approximate \vec{u} as

$$\vec{u} \approx \Theta_{I_{Pr}, I_{Tr}} \Theta_{I_{Tr}, I_{Tr}}^{-1} \vec{g}. \tag{5.1}$$

This is a classical technique for the solution of partial differential equations, known as single layer boundary element methods (Sauter and Schwab, 2011). However, it can also be seen as Gaussian process regression with u being the conditional mean of a Gaussian process with covariance function G , conditional on the values of the process on $\partial\Omega$. Similarly it can be shown that the zero boundary value Green's function is given by the posterior covariance of the same process.



Figure 9: We recursively divide each panel of $\partial\Omega$. The basis functions on finer levels are constructed as linear combinations of indicator functions that are orthogonal to functions on coarser levels.

The Laplace operator in three dimensions does not satisfy $s > d/2$ (cf. Section 3.3.2). Therefore, the variance of pointwise evaluations at $x \in \mathbb{R}^3$ given by $G_{\mathbb{R}^3}(x, x)$ is infinite and we cannot use $\{\phi_i\}_{i \in I_{\text{Pr}}}$ to be Dirac-functions as in other parts of this work.

Instead, we recursively subdivide the boundary $\partial\Omega$ and use Haar-type wavelets as in Schäfer et al. (2017, Ex. 3.2) for $\{\phi_i\}_{i \in I_{\text{Tr}}}$. For our numerical experiments we will consider $\Omega := [0, 1]^3$ to be the three-dimensional unit cube. On each face of $\partial\Omega$, we then obtain a multiresolution basis by hierarchical subdivision as shown in Figure 5.4. In this case, the equivalent of a maximin ordering is an ordering from coarser to finer levels, with an arbitrary ordering within each level. We construct our sparsity pattern as

$$\mathcal{S}_{\prec, l_j, \rho} := \{ (i, j) : i \succeq j, \text{dist}(x_i, x_j) \leq \rho l_j + \sqrt{2}(l_i + l_j) \},$$

where for $i \in I_{\text{Tr}}$, x_i is defined as the center of the support of ϕ_i and l_i as half of the side-length of the (quadratic) support of ϕ_i . The addition of $\sqrt{2}(l_i + l_j)$ to the right-hand side ensures that the entries corresponding to neighboring basis functions are always added to the sparsity pattern.

We construct a solution u of the Laplace equation in Ω as the sum over $N_c = 2000$ charges with random signs $\{s_i\}_{1 \leq i \leq N_c}$ located at points $\{c_i\}_{1 \leq i \leq N_c}$. We then pick a set of N_{Pr} points $\{x_i\}_{i \in I_{\text{Pr}}}$ inside of Ω and try to predict the values $\{u(x_i)\}_{i \in I_{\text{Pr}}}$ using Equation (5.1) and the method described in Section 4.3.2. We compare the computational time, number of entries in the sparsity pattern, and mean accuracy of the approximate method for $\rho \in \{1.0, 2.0, 3.0\}$, as well as the exact solution of the linear system. We use different levels of discretization $q \in \{3, \dots, 8\}$, leading to a spatial resolution of up to 2^{-8} . As shown in Figure 5.4, even using $\rho = 1.0$ leads to near-optimal accuracy, at a greatly reduced computational cost.

There exists a rich literature on the numerical solution of boundary element equations (Sauter and Schwab, 2011) and we are not yet claiming improvement over the state of the art. Presently, the majority of the computational time is spent computing the matrix entries of $\Theta_{\text{Tr}, \text{Tr}}$. In order to compete with the state of the art in terms of wall-clock times, we would need to implement more efficient quadrature rules which is beyond the scope of this paper. Due to the embarrassing parallelism of our method together with the high accuracy obtained even for small values of ρ , we hope that it will become a useful tool for solving boundary integral equations, but we defer a detailed study to future work.

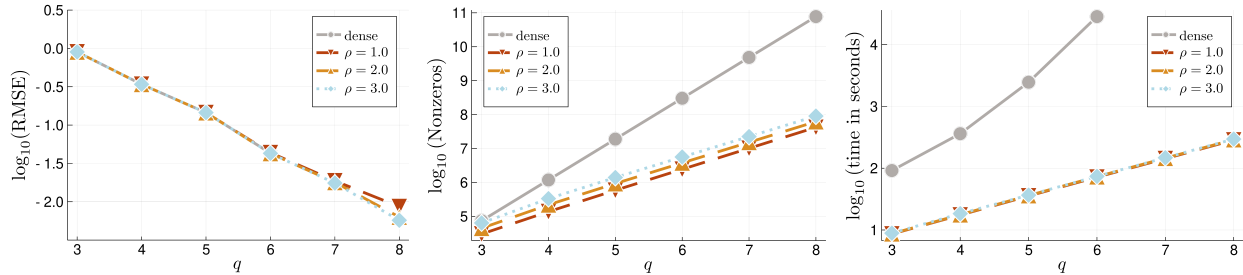


Figure 10: Accuracy and computational complexity in boundary value problem. We compare the root mean square error, number of nonzeros of sparsity pattern, and the computational time for the exact boundary element method and using our approximation for $\rho \in \{1, 2, 3\}$. The dense solution is prohibitively expensive for $q > 6$, which is why accuracy and computational time for these cases are missing. The reason that the computational time is hardly affected by different choices of ρ is due to the fact that entries $(\Theta_{\text{Tr,Tr}})_{ij}$ for nearby ϕ_i, ϕ_j are significantly more expensive to compute than for distant ones when using an off-the-shelf adaptive quadrature rule. The computations were performed on 32 threads of an Intel[®] Skylake[™] CPU with 2.10GHz and 192 GB of RAM.

6 Conclusions

In this work, we have shown that, surprisingly, the optimal (in KL-divergence) inverse Cholesky factor of a positive definite matrix, subject to a sparsity pattern, can be computed in closed form. In the special case of Green’s matrices of elliptic boundary value problems in d dimensions, we show that by applying this method to the elimination orderings and sparsity patterns proposed by Schäfer et al. (2017), one can compute the sparse inverse Cholesky factor with accuracy ϵ in computational complexity $\mathcal{O}(N \log^{2d}(N/\epsilon))$ using only $\mathcal{O}(N \log^d(N/\epsilon))$ entries of the dense Green’s matrix. This improves upon the state of the art in this classical problem. We also propose a variety of improvements, capitalizing on the improved stability, parallelism, and memory footprint of our method. Finally, we show how to extend our approximation to the setting with additive noise, resolving a major open problem in spatial statistics.

Acknowledgements

FS and HO gratefully acknowledge support by the Air Force Office of Scientific Research under award number FA9550-18-1-0271 (Games for Computation and Learning), and the Office of Naval Research under award N00014-18-1-2363 (Toward scalable universal solvers for linear systems). MK’s research was partially supported by National Science Foundation (NSF) CAREER grant DMS-1654083. The computations in Section 5.4 were conducted on the Caltech High Performance Cluster partially supported by a grant from the Gordon and Betty Moore Foundation.

References

S. Ambikasaran and E. Darve. An $\mathcal{O}(n \log n)$ fast direct solver for partial hierarchically semi-separable matrices. *Journal of Scientific Computing*, 57(3):477–501, 2013.

- F. R. Bach and M. I. Jordan. Kernel independent component analysis. *J. Mach. Learn. Res.*, 3(1): 1–48, 2003. doi:10.1162/153244303768966085.
- S. Banerjee, A. E. Gelfand, A. O. Finley, and H. Sang. Gaussian predictive process models for large spatial data sets. *J. R. Stat. Soc. Ser. B Stat. Methodol.*, 70(4):825–848, 2008. doi:10.1111/j.1467-9868.2008.00663.x.
- R. Baptista, O. Zahm, and Y. Marzouk. Adaptive transport maps for high-dimensional density estimation. (in preparation), 2020.
- M. Benzi and M. Tuma. A comparative study of sparse approximate inverse preconditioners. *Appl. Numer. Math.*, 30(2-3):305–340, 1999. ISSN 0168-9274. doi:10.1016/S0168-9274(98)00118-4. URL [https://doi.org/10.1016/S0168-9274\(98\)00118-4](https://doi.org/10.1016/S0168-9274(98)00118-4). Iterative methods and preconditioners (Berlin, 1997).
- G. Beylkin, R. Coifman, and V. Rokhlin. Fast wavelet transforms and numerical algorithms. I. *Comm. Pure Appl. Math.*, 44(2):141–183, 1991. doi:10.1002/cpa.3160440202.
- S. Chandrasekaran, M. Gu, and T. Pals. Fast and stable algorithms for hierarchically semi-separable representations. *submitted for publication*, 2004.
- A. Datta, S. Banerjee, A. O. Finley, and A. E. Gelfand. Hierarchical nearest-neighbor Gaussian process models for large geostatistical datasets. *Journal of the American Statistical Association*, 111(514):800–812, 2016.
- S. Eguchi and J. Copas. Interpreting Kullback-Leibler divergence with the Neyman-Pearson lemma. *J. Multivariate Anal.*, 97(9):2034–2040, 2006. ISSN 0047-259X. doi:10.1016/j.jmva.2006.03.007. URL <https://doi.org/10.1016/j.jmva.2006.03.007>.
- A. Y. Eremin, L. Y. Kolotilina, and A. A. Nikishin. Factorized sparse approximate inverse preconditionings. III. Iterative construction of preconditionings. *Zap. Nauchn. Sem. S.-Peterburg. Otdel. Mat. Inst. Steklov. (POMI)*, 248(Chisl. Metody i Vopr. Organ. Vychisl. 13):17–48, 247, 1998. ISSN 0373-2703. doi:10.1007/BF02672769. URL <https://doi.org/10.1007/BF02672769>.
- M. Ferronato, C. Janna, and G. Gambolati. A novel factorized sparse approximate inverse preconditioner with supernodes. *Procedia Computer Science*, 51:266–275, 2015.
- S. Fine and K. Scheinberg. Efficient SVM training using low-rank kernel representations. *J. Mach. Learn. Res.*, 2:243–264, 2001.
- C. Fowlkes, S. Belongie, F. Chung, and J. Malik. Spectral grouping using the Nyström method. *IEEE Trans. Pattern Anal. Mach. Intell.*, 26(2):214–225, 2004.
- R. Furrer, M. G. Genton, and D. Nychka. Covariance tapering for interpolation of large spatial datasets. *J. Comput. Graph. Statist.*, 15(3):502–523, 2006. doi:10.1198/106186006X132178.
- L. Greengard and V. Rokhlin. A fast algorithm for particle simulations. *J. Comput. Phys.*, 73(2): 325–348, 1987. doi:10.1016/0021-9991(87)90140-9.
- J. Guinness. Permutation methods for sharpening Gaussian process approximations. *Technometrics*, 60(4):415–429, 2018. doi:10.1080/00401706.2018.1437476.
- A. Gutjahr, B. Bullard, and S. Hatch. General joint conditional simulations using a fast fourier transform method. *Mathematical Geology*, 29(3):361–389, 1997.
- W. Hackbusch. A sparse matrix arithmetic based on \mathcal{H} -matrices. I. Introduction to \mathcal{H} -matrices. *Computing*, 62(2):89–108, 1999. doi:10.1007/s006070050015.
- W. Hackbusch and S. Börm. Data-sparse approximation by adaptive \mathcal{H}^2 -matrices. *Computing*, 69(1):1–35, 2002. doi:10.1007/s00607-002-1450-4.
- W. Hackbusch and B. N. Khoromskij. A sparse \mathcal{H} -matrix arithmetic. II. Application to multi-dimensional problems. *Computing*, 64(1):21–47, 2000.

- K. L. Ho and L. Ying. Hierarchical interpolative factorization for elliptic operators: integral equations. *Comm. Pure Appl. Math.*, 69(7):1314–1353, 2016. ISSN 0010-3640. doi:10.1002/cpa.21577. URL <https://doi.org/10.1002/cpa.21577>.
- T. Hofmann, B. Schölkopf, and A. J. Smola. Kernel methods in machine learning. *Ann. Statist.*, 36(3):1171–1220, 2008. ISSN 0090-5364. doi:10.1214/009053607000000677.
- W. James and C. Stein. Estimation with quadratic loss. *Proceedings of the Fourth Berkeley Symposium on Mathematical Statistics and Probability*, 1:361–379, 1961. doi:10.1177/0278364907080252.
- I. E. Kaporin. An alternative approach to the estimation of the number of iterations in the conjugate gradient method. In *Numerical methods and software (Russian)*, pages 55–72. Akad. Nauk SSSR, Otdel Vychisl. Mat., Moscow, 1990.
- M. Katzfuss. A multi-resolution approximation for massive spatial datasets. *J. Amer. Stat. Assoc.*, 2016. doi:10.1080/01621459.2015.1123632.
- M. Katzfuss and W. Gong. A class of multi-resolution approximations for large spatial datasets. *Statistica Sinica*, forthcoming, 2019.
- M. Katzfuss and J. Guinness. A general framework for Vecchia approximations of Gaussian processes. *Statistical Science*, forthcoming, 2019. URL <http://arxiv.org/abs/1708.06302>.
- M. Katzfuss, J. Guinness, W. Gong, and D. Zilber. Vecchia approximations of Gaussian-process predictions. *arXiv:1805.03309*, 2018.
- C. G. Kaufman, M. J. Schervish, and D. W. Nychka. Covariance tapering for likelihood-based estimation in large spatial data sets. *Journal of the American Statistical Association*, 103(484):1545–1555, 2008.
- L. Y. Kolotilina and A. Y. Yeremin. Factorized sparse approximate inverse preconditionings. I. Theory. *SIAM J. Matrix Anal. Appl.*, 14(1):45–58, 1993. ISSN 0895-4798. doi:10.1137/0614004. URL <https://doi.org/10.1137/0614004>.
- R. Kornhuber and H. Yserentant. An analysis of a class of variational multiscale methods based on subspace decomposition, 2016. arXiv:1608.04081.
- F. Lindgren, H. Rue, and J. Lindström. An explicit link between Gaussian fields and Gaussian Markov random fields: the stochastic partial differential equation approach. *J. R. Stat. Soc. Ser. B Stat. Methodol.*, 73(4):423–498, 2011. doi:10.1111/j.1467-9868.2011.00777.x.
- A. Målqvist and D. Peterseim. Localization of elliptic multiscale problems. *Mathematics of Computation*, 83(290):2583–2603, 2014.
- Y. Marzouk, T. Moselhy, M. Parno, and A. Spantini. Sampling via measure transport: an introduction. In *Handbook of uncertainty quantification. Vol. 1, 2, 3*, pages 785–825. Springer, Cham, 2017.
- H. Owhadi and C. Scovel. Universal scalable robust solvers from computational information games and fast eigenspace adapted multiresolution analysis, 2017. arXiv:1703.10761.
- H. Owhadi and C. Scovel. *Operator Adapted Wavelets, Fast Solvers, and Numerical Homogenization, from a game theoretic approach to numerical approximation and algorithm design*. Cambridge Monographs on Applied and Computational Mathematics. Cambridge University Press, 2019.
- J. Quiñonero-Candela and C. E. Rasmussen. A unifying view of sparse approximate Gaussian process regression. *J. Mach. Learn. Res.*, 6(Dec):1939–1959, 2005.
- C. E. Rasmussen and C. K. I. Williams. *Gaussian Processes for Machine Learning*. Adaptive Computation and Machine Learning. MIT Press, Cambridge, MA, 2006.

- L. Roininen, M. S. Lehtinen, S. Lasanen, M. Orispää, and M. Markkanen. Correlation priors. *Inverse Probl. Imaging*, 5(1):167–184, 2011. doi:10.3934/ipi.2011.5.167.
- L. Roininen, P. Piironen, and M. Lehtinen. Constructing continuous stationary covariances as limits of the second-order stochastic difference equations. *Inverse Probl. Imaging*, 7(2):611–647, 2013. doi:10.3934/ipi.2013.7.611.
- L. Roininen, J. M. J. Huttunen, and S. Lasanen. Whittle-Matérn priors for Bayesian statistical inversion with applications in electrical impedance tomography. *Inverse Probl. Imaging*, 8(2): 561–586, 2014. doi:10.3934/ipi.2014.8.561.
- H. Sang and J. Z. Huang. A full scale approximation of covariance functions for large spatial data sets. *J. R. Stat. Soc. Ser. B. Stat. Methodol.*, 74(1):111–132, 2012. doi:10.1111/j.1467-9868.2011.01007.x.
- S. A. Sauter and C. Schwab. *Boundary Element Methods*, volume 39 of *Springer Series in Computational Mathematics*. Springer-Verlag, Berlin Heidelberg, 2011. doi:10.1007/978-3-540-68093-2.
- F. Schäfer, T. J. Sullivan, and H. Owhadi. Compression, inversion, and approximate PCA of dense kernel matrices at near-linear computational complexity. *arXiv:1706.02205*, 2017. URL <http://arxiv.org/abs/1706.02205>.
- A. Schwaighofer and V. Tresp. Transductive and inductive methods for approximate Gaussian process regression. In S. Becker, S. Thrun, and K. Obermayer, editors, *Advances in Neural Information Processing Systems 15*, pages 977–984. MIT Press, 2003.
- A. J. Smola and P. L. Bartlett. Sparse greedy Gaussian process regression. In *Advances in Neural Information Processing Systems*, pages 619–625, 2001.
- E. Snelson and Z. Ghahramani. Sparse Gaussian processes using pseudo-inputs. In Y. Weiss, P. B. Schölkopf, and J. C. Platt, editors, *Advances in Neural Information Processing Systems 18*, pages 1257–1264. MIT Press, 2006. URL <http://papers.nips.cc/paper/2857-sparse-gaussian-processes-using-pseudo-inputs.pdf>.
- M. L. Stein. The screening effect in kriging. *Ann. Statist.*, 30(1):298–323, 2002. doi:10.1214/aos/1015362194.
- M. L. Stein. 2010 Rietz Lecture: When does the screening effect hold? *Ann. Statist.*, 39(6):2795–2819, 2011. ISSN 0090-5364. doi:10.1214/11-AOS909. URL <https://doi.org/10.1214/11-AOS909>.
- M. L. Stein, Z. Chi, and L. J. Welty. Approximating likelihoods for large spatial data sets. *J. R. Stat. Soc. Ser. B Stat. Methodol.*, 66(2):275–296, 2004. doi:10.1046/j.1369-7412.2003.05512.x.
- Y. Sun and M. L. Stein. Statistically and computationally efficient estimating equations for large spatial datasets. *Journal of Computational and Graphical Statistics*, 25(1):187–208, 2016. ISSN 1061-8600. doi:10.1080/10618600.2014.975230.
- A. Vecchia. Estimation and model identification for continuous spatial processes. *Journal of the Royal Statistical Society, Series B*, 50(2):297–312, 1988.
- C. K. I. Williams and M. Seeger. Using the Nyström method to speed up kernel machines. In T. K. Leen, T. G. Dietterich, and V. Tresp, editors, *Advances in Neural Information Processing Systems 13*, pages 682–688. MIT Press, 2001. URL <http://papers.nips.cc/paper/1866-using-the-nystrom-method-to-speed-up-kernel-machines.pdf>.

A Computation of the KL-minimizer

A.1 Computation without aggregation

As in the main part, write I for the set indexing the degrees of freedom, \prec for a r -reverse-maximin ordering, and $S = S_{\prec, l, \rho}$ for the associated sparsity pattern (which we assume to be fixed). Unless explicitly mentioned, we assume all matrices have rows and columns ordered according to \prec . For $k \in I$, we then write $s_k := \{(i, k) : k \preceq i, (i, k) \in S\}$ for the sparsity set of the k -th column $L_{:,k}$ of L . As before, \mathbf{e}_1 is a vector of variable length that has 1 as its first entry and 0 everywhere else, and analogously \mathbf{e}_k is the vector that is 1 on the k -th coordinate and zero everywhere else.

Proof of Theorem 2.1. By using the formula for the KL-divergence of two Gaussian random variables in (2.1), we obtain

$$\begin{aligned} L &= \operatorname{argmin}_{\hat{L} \in \mathcal{S}} \left(\operatorname{trace}(\hat{L}\hat{L}^\top \Theta) - \log \det(\hat{L}\hat{L}^\top) - \log \det(\Theta) - N \right) \\ &= \operatorname{argmin}_{\hat{L} \in \mathcal{S}} \left(\operatorname{trace}(\hat{L}^\top \Theta \hat{L}) - \log \det(\hat{L}\hat{L}^\top) \right) \\ &= \operatorname{argmin}_{\hat{L} \in \mathcal{S}} \sum_{k=1}^N \left(\hat{L}_{s_k, k}^\top \Theta_{s_k, s_k} \hat{L}_{s_k, k} - 2 \log(\hat{L}_{k, k}) \right). \end{aligned}$$

The k -th summand depends only on the k -th column of \hat{L} . Thus, taking the derivative with respect to the k -th column of L and setting it to zero, we obtain $\Theta_{s_k, s_k} \hat{L}_{s_k, k} = \frac{\mathbf{e}_1}{\hat{L}_{k, k}} \Leftrightarrow \hat{L}_{s_k, k} = \frac{\Theta_{s_k, s_k}^{-1} \mathbf{e}_1}{\hat{L}_{k, k}}$. Therefore, $\hat{L}_{s_k, k}$ can be written as $\lambda \Theta_{s_k, s_k}^{-1} \mathbf{e}_1$ for a $\lambda \in \mathbb{R}$. By plugging this ansatz into the equation, we obtain $\lambda = \sqrt{(\Theta_{s_k, s_k}^{-1} \mathbf{e}_1)_1} = \sqrt{\mathbf{e}_1^\top \Theta_{s_k, s_k}^{-1} \mathbf{e}_1}$ and hence Equation (2.3). By using dense Cholesky factorization to invert the Θ_{s_k, s_k} , the right-hand side of Equation (2.3) can be computed in computational complexity $\mathcal{O}(\#(s_k)^2)$ in space and $\mathcal{O}(\#(s_k)^3)$ in time, from which follows the result. \square

Algorithm 1 is a direct implementation of the above formula.

A.2 Computation for the aggregated sparsity pattern

We first introduce some additional notation, defined in terms of an r -maximin ordering \prec and aggregated sparsity set $S = \tilde{S}_{\prec, l, \rho, \lambda}$, which we assume to be fixed. Unless explicitly mentioned, we assume all matrices to have rows and columns ordered according to \prec . As before, I is the index set keeping track over the degrees of freedom and \tilde{I} is index set indexing the supernodes. For a matrix A and sets of indices \tilde{i} and \tilde{j} , we denote as the $A_{\tilde{i}, \tilde{j}}$ the submatrix obtained by restricting the indices of A to \tilde{i} and \tilde{j} , and as $A_{\tilde{i}, \cdot}$ ($A_{\cdot, \tilde{j}}$) the matrix obtained by only restricting the row (column) indices. We adopt the convention of indexing having precedence over inversion, i.e. $A_{\tilde{i}, \tilde{j}}^{-1} = (A_{\tilde{i}, \tilde{j}})^{-1}$. For a supernode $\tilde{k} \in \tilde{I}$ and a degree of freedom $j \in I$, we write $j \in \tilde{k}$ if there exists a $k \rightsquigarrow \tilde{k}$ such that $k \preceq j$ and $(k, j) \in S$, and we accordingly form submatrices $A_{\tilde{i}, \tilde{j}} := (A_{ij})_{i \in \tilde{i}, j \in \tilde{j}}$. Note that by definition of the supernodes, we have $s_k \subset \tilde{k}$ for all $k \rightsquigarrow \tilde{k}$. Since we assume the sparsity pattern S to contain the diagonal, we furthermore have $k \rightsquigarrow \tilde{k} \Rightarrow k \in \tilde{k}$.

We first show how to efficiently compute the inverse Cholesky factor for the aggregated sparsity pattern (as has been observed before by Ferronato et al., 2015, and Guinness, 2018). For $\tilde{k} \in \tilde{I}$, we define $U^{\tilde{k}}$ as the unique upper triangular matrix such that $\Theta_{\tilde{k},\tilde{k}} = U^{\tilde{k}}U^{\tilde{k},\top}$. $U^{\tilde{k}}$ can be computed in complexity $\mathcal{O}((\#\tilde{k})^3)$ in time and $\mathcal{O}((\#\tilde{k})^2)$ in space by computing the Cholesky factorization of $\Theta_{\tilde{k},\tilde{k}}$ after reverting the ordering of its rows and columns, and then reverting the order of the rows and columns of the resulting Cholesky factor. The upper triangular structure of $U^{\tilde{k}}$ implies the following properties

$$\Theta_{s_k,s_k} = U_{s_k,s_k}^{\tilde{k}} U_{s_k,s_k}^{\tilde{k},\top}, \quad U_{s_k,s_k}^{\tilde{k},-1} \mathbf{1} = \frac{1}{U_{kk}^{\tilde{k}}} \mathbf{e}_1, \quad U_{s_k,s_k}^{\tilde{k},-\top} \mathbf{1} = \left(U_{s_k,s_k}^{\tilde{k},-\top} \mathbf{e}_k \right)_{s_k,s_k}, \quad U_{s_k,s_k}^{\tilde{k},-1} v_{s_k} = \left(U_{s_k,s_k}^{\tilde{k},-1} v \right)_{s_k}, \quad (\text{A.1})$$

where $v \in \mathbb{R}^{\tilde{k}}$ is chosen arbitrarily. For any $k \rightsquigarrow \tilde{k}$, the first three properties above imply

$$L_{:,k}^\rho = \frac{\Theta_{s_k}^{-1} \mathbf{e}_1}{\sqrt{\mathbf{e}_1^\top \Theta_{s_k}^{-1} \mathbf{e}_1}} = U_{s_k,s_k}^{\tilde{k},-\top} \mathbf{e}_1 = U_{s_k,s_k}^{\tilde{k},-\top} \mathbf{e}_k.$$

Thus, computing the columns $L_{:,k}$ for all $k \rightsquigarrow \tilde{k}$ has computational complexity $\mathcal{O}((\#\tilde{k})^3)$ in time and $\mathcal{O}((\#\tilde{k})^2)$ in space. Algorithm 2 implements the formulae derived above.

A.3 GP regression in $\mathcal{O}(N + \rho^{2\tilde{d}})$ space complexity

As mentioned in Section 4.2, for many important operations arising in GP regression, the inverse-Cholesky factors L of the training covariance matrix need never be formed in full. Instead, matrix-vector multiplies with L or L^\top , as well as the computation of the log-determinant of L can be performed by computing the columns of L in an arbitrary order, using them to update the result, and deleting them again. For the example of computing the posterior mean μ and covariance C , this is done in Algorithms 5 (without aggregation) and 6 (with aggregation). In Section B, we show how to compute the reverse maximin ordering and aggregated sparsity pattern in space complexity $\mathcal{O}(N + \rho^{\tilde{d}})$, thus allowing the entire algorithm to be run in space complexity $\mathcal{O}(N + \rho^{\tilde{d}})$ when using the aggregated sparsity pattern.

B Computation of the ordering and sparsity pattern

We will now explain how to compute the ordering and sparsity pattern described in Section 3, using only near-linearly many evaluations of an oracle $\text{dist}(i, j)$ that returns the distance between the points x_i and x_j . To do so efficiently in general, we need to impose a mild additional assumption on the dataset (cf. Schäfer et al., 2017).

Condition B.1 (Polynomial Scaling). There exists a polynomial \mathbf{p} for which

$$\frac{\max_{i \neq j \in I} \text{dist}(x_i, x_j)}{\min_{i \neq j \in I} \text{dist}(x_i, x_j)} \leq \mathbf{p}(N).$$

Under Conditions 3.2 and B.1, Schäfer et al. (2017, Alg. 3) allows us to compute the maximin ordering \prec and sparsity pattern $\{(i, j) : \text{dist}(x_i, x_j) \leq \rho \max(l_i, l_j)\}$ in computational complexity $\mathcal{O}(N \log(N) \rho^{\tilde{d}})$ in space and time. The resulting pattern is larger than the sparsity pattern $S_{\prec, \rho}$

Algorithm 5: Without aggregation	Algorithm 6: With aggregation
<p>Data: $G, \{x_i\}_{i \in I}, \prec, S_{\prec, l, \rho}$ Result: Cond. mean μ and covariance C</p> <pre> for $k \in I_{Pr}$ do $\mu_k \leftarrow 0$; for $i \in I_{Tr}, j \in I_{Pr}$ do $(\Theta_{Tr, Pr})_{ij} \leftarrow G(x_i, x_j)$; for $i \in I_{Pr}, j \in I_{Pr}$ do $(\Theta_{Pr, Pr})_{ij} \leftarrow G(x_i, x_j)$; for $k \in I_{Tr}$ do for $i, j \in s_k$ do $(\Theta_{s_k, s_k})_{ij} \leftarrow G(x_i, x_j)$; $v \leftarrow \Theta_{s_k, s_k}^{-1} \mathbf{e}_k$; $v \leftarrow v/v_k$; $\mu_{k,:} \leftarrow \mu_{k,:} + v_k \Theta_{k, Pr}$; $B_{k,:} \leftarrow v^\top \Theta_{Tr, Pr}$; $C \leftarrow \Theta_{Pr, Pr} - B^\top B$; return μ, C; </pre>	<p>Data: $G, \{x_i\}_{i \in I}, \prec, S_{\prec, l, \rho, \lambda}$ Result: Cond. mean μ and covariance C</p> <pre> for $k \in I_{Pr}$ do $\mu_k \leftarrow 0$; for $i \in I_{Tr}, j \in I_{Pr}$ do $(\Theta_{Tr, Pr})_{ij} \leftarrow G(x_i, x_j)$; for $i \in I_{Pr}, j \in I_{Pr}$ do $(\Theta_{Pr, Pr})_{ij} \leftarrow G(x_i, x_j)$; for $\tilde{k} \in \tilde{I}$ do for $i, j \in s_{\tilde{k}}$ do $(\Theta_{s_{\tilde{k}}, s_{\tilde{k}}})_{ij} \leftarrow G(x_i, x_j)$; $U \leftarrow P^\dagger \text{chol}(P^\dagger K_{s_{\tilde{k}}, s_{\tilde{k}}} P^\dagger) P^\dagger$; for $k \rightsquigarrow \tilde{k}$ do $v \leftarrow U^{-\top} \mathbf{e}_k$; $\mu_{k,:} \leftarrow \mu_{k,:} + v_k \Theta_{k, Pr}$; $B_{k,:} \leftarrow v^\top \Theta_{Tr, Pr}$; $C \leftarrow \Theta_{Pr, Pr} - B^\top B$; return μ, C; </pre>

Figure 11: Prediction and uncertainty quantification using KL-minimization with and without aggregation in $\mathcal{O}(N + \rho^{2d})$ memory complexity

introduced in Section 3.1, which can thus be obtained by truncating the pattern obtained by Schäfer et al. (2017, Alg. 3). By performing the truncation of the sets of children and parents c, p as used by Schäfer et al. (2017, Alg. 3) during execution of the algorithm, as opposed to truncating the sparsity pattern after execution of the algorithm, the space complexity for obtaining \prec and $S_{\prec, l, \rho}$ can be reduced to $\mathcal{O}(N\rho^{\tilde{d}})$. Algorithm 7 is a minor modification of Schäfer et al. (2017, Alg. 3) that performs such a truncation.

Theorem B.2 (Variant of Schäfer et al. (2017, Thm. A.5)). *Let $\Omega = \mathbb{R}^d$ and $\rho \geq 2$. Algorithm 7 computes the reverse maximin ordering \prec and sparsity pattern $S_{\prec, l, \rho}$ in computational complexity $C\rho^{\tilde{d}}N$ in space and $CN \log(N)\rho^{\tilde{d}}(\log N + C_{\text{dist}})$ in time. Here, $C = C(\tilde{d}, C_{\tilde{d}}, \mathbf{p})$ depends only on the constants appearing in Conditions 3.2 and B.1, and C_{dist} is the cost of evaluating dist .*

Proof. The proof is essentially the same as the proof of Schäfer et al. (2017, Thm. A.5). \square

Similarly, the proof of Schäfer et al. (2017, Thm. A.2) can be adapted to show that in the setting of Theorem 3.5, there exists a constant C depending only on d, Ω , and δ , such that for $\rho > C$, Algorithm 7 computes the maximin ordering in computational complexity $CN(\log(N)\rho^d + C_{\text{dist}_\Omega})$ in time and $CN\rho^d$ in space, where C_{dist_Ω} is an upper bound on the complexity of computing the distance of an arbitrary point $x \in \Omega$ to $\partial\Omega$.

We furthermore note that a reverse r -maximin ordering with $r < 1$ (see Definition 3.1) can be computed in computational complexity $\mathcal{O}(N \log(N))$ by quantizing the values of $(\log(l_i))_{i \in I}$ in multiples of $\log(r)$, which avoids the complexity incurred by the restoration of the heap property in Line 20 of Schäfer et al. (2017, Alg. 3).

As described in Section 3.2, the aggregated sparsity pattern $S_{\prec, l, \rho, \lambda}$ can be computed efficiently from $S_{\prec, l, \rho}$. However, forming the pattern $S_{\prec, l, \rho}$ using a variant of Schäfer et al. (2017, Alg. 3) has

complexity $\mathcal{O}(N \log(N) \rho^{\tilde{d}})$ in time and $\mathcal{O}(N \rho^{\tilde{d}})$ in space, while the aggregated pattern $S_{\prec, l, \rho, \lambda}$ only has space complexity $\mathcal{O}(N)$, begging the question if this computational complexity can be improved. Let $\{s_{\tilde{i}}\}_{\tilde{i} \in \tilde{I}}$ be the supernodes as constructed in Section 3.2 and identify each supernodal index \tilde{i} with the first (w.r.t. \prec) index $i \in I$ such that $i \rightsquigarrow \tilde{i}$. We then define

$$\bar{S}_{\prec, l, \rho, \lambda} := \bigcup_{\tilde{i} \in \tilde{I}} \{(i, j) : i \preceq j, i \rightsquigarrow \tilde{i}, \text{dist}(x_{\tilde{i}}, x_j) \leq \rho(1 + \lambda)\tilde{i}\}.$$

Algorithm 8 allows us to construct the sparsity pattern $\bar{S}_{\prec, l, \rho, \lambda} \supset \tilde{S}_{\prec, l, \rho, \lambda}$ in complexity $\mathcal{O}(N \log(N))$ in time and $\mathcal{O}(N)$ in space, given \prec and l . In this algorithm, we will implement supernodes as pairs of arrays of indices $\sigma = (\sigma_m, \sigma_n)$. This encodes the relationship between all indices in σ_m (the *parents*) and all indices in σ_n (the *children*). Naively, this would require $\mathcal{O}(\#\sigma_m \#\sigma_n)$ space complexity, but by storing the entries of σ_m and σ_n , the complexity is reduced to $\mathcal{O}(\#\sigma_m + \#\sigma_n)$ space complexity, which improves the asymptotic computational complexity.

Theorem B.3. *Let the $\{x_i\}_{i \in I}$ satisfy Condition 3.2 with \tilde{d} and $C_{\tilde{d}}$, Condition 3.3 with constant C_{regref} , and Condition B.1 with \mathbf{p} and let $\lambda > 1$. Then there exists a constant $C = C_{\tilde{d}, C_{\tilde{d}}, C_{\text{regref}}, \mathbf{p}, \lambda}$ such that Algorithm 8 can compute $\bar{S}_{\prec, l, \rho, \lambda}$ in computational complexity $CC_{\text{dist}} N \log(N)$ in time and CN in space and $\tilde{S}_{\prec, l, \rho, \lambda}$ in computational complexity $CC_{\text{dist}} N(\log(N) + \rho^{\tilde{d}})$ in time and CN in space.*

Proof. To establish correctness, the main observation is that after every application of Algorithm 10, each degree of freedom i can be found in exactly one of the supernodes $\sigma \in \mathcal{N}$. Furthermore, each $\sigma \in \mathcal{N}$ has a root $\sqrt{\sigma} \in I$ such that

1. $\sqrt{\sigma} \in \sigma_n, \sigma_m$,
2. $j \in \sigma_m \Rightarrow \text{dist}(\sqrt{\sigma}, j) \leq \rho\lambda r$,
3. $j \in \sigma_n \Leftrightarrow \text{dist}(\sqrt{\sigma}, j) \leq 2\rho\lambda r$,
4. $\sigma \neq \bar{\sigma} \Rightarrow \text{dist}(\sqrt{\sigma}, \sqrt{\bar{\sigma}}) > \rho\lambda r$.

The main reason why the above could fail to hold true is that the inner for loop does not range over all $j \in I$, but only over those in σ_n . However, at the first occurrence of Algorithm 10 we have $\sigma_n = I$ leading to the observations to hold true. For subsequent calls, we can show the invariance of these properties by induction. The set \mathcal{N}^{\geq} is obtained from the set \mathcal{N} by only selecting the points in a certain range of length scales. Therefore, after completion of the while-loop of Algorithm 8, every $i \in I$ is contained in at least one of the $\{\sigma_m\}_{\sigma \in \mathcal{N}^{\geq}}$, and for $i \rightsquigarrow \sigma \in \mathcal{N}^{\geq}$, we have $\{j : (i, j) \in \bar{S}\} \subset \sigma_n$. Thus, the for-loop of Algorithm 8 indeed computes \bar{S} . Since $\tilde{S}_{\prec, l, \rho, \lambda} \subset \bar{S}_{\prec, l, \rho, \lambda}$, Algorithm 9 correctly recovers $\tilde{S}_{\prec, l, \rho, \lambda}$.

We begin by analyzing the computational complexity of the while-loop of Algorithm 8. We first note that at every execution of the loop, r is divided by λ . Thus, Condition B.1 implies that the loop is entered at most $C \log(N)$ times. We now claim that that the time complexity of Algorithm 10 is bounded above by $CC_{\text{dist}} N$. To this end it is enough to upper-bound the number of points i for which a given index can be picked as index j in the while-loop of Algorithm 10. By Property 2, for this to happen we need $\text{dist}(i, \sqrt{\sigma}) \leq \rho\lambda r$ and $\text{dist}(j, \sqrt{\sigma}) \leq 2\rho\lambda r$ and hence, by the triangle inequality, $\text{dist}(i, j) \leq 3\rho\lambda r$. On the other hand, i can not be in J already, which means that any two distinct i_1, i_2 have to satisfy $\text{dist}(i_1, i_2) > \rho\lambda r$. By Condition 3.2, we conclude that the maximum number of indices i for which a given index j gets picked is bounded above by a constant C that depends of $C_{\tilde{d}}$ and d . This upper bounds the computational complexity of the while-loop

in Algorithm 10 by CN . The computational complexity of the outermost for-loop of Algorithm 10 can be bounded by CN , by a similar argument. Summarizing the above, we have upper-bounded the time complexity of the while-loop in Algorithm 8 by $CN \log(N)$. In order to bound the space complexity of the while-loop, we need to ensure that the size of \mathcal{N}^{\geq} is bounded above as CN . To this end, we notice that by arguments similar to the above, one can show that at all times, the number $\max_{i \in I} \#\{\sigma \in \mathcal{N} : i \in \sigma_m \text{ or } i \in \sigma_N\}$ is bounded from above by a constant C . By using Condition 3.3, we can show that the space complexity of \mathcal{N}^{\geq} is bounded by CN . By ways of similar ball packing arguments, the complexity of the outer for-loop of Algorithm 8 can be bounded by CN , as well. The complexity of Algorithm 9 is bounded by $CN\rho^{\bar{d}}$, the number of entries of the sparsity pattern \bar{S} , since it iterates over all entries of \bar{S} . \square

C Postponed proofs

C.1 Computational complexity

Proof of Theorem 3.4. We begin by showing that the number of nonzero entries of an arbitrary column of $S_{\prec, l, \rho}$ is bounded above as $C\rho^{\bar{d}}$. Considering the i -th column, the reverse r -maximin ordering ensures that for all $j, k \succ i$, we have $\text{dist}(x_j, x_i) \geq rl_i$. Since for all $(i, j) \in S_{\prec, l, \rho}$ we have $i \prec j$ and $\text{dist}(x_i, x_j) \leq \rho l_i$, Condition 3.2 implies that $\#\{j : (i, j) \in S_{\prec, l, \rho}\} \leq C_{\bar{d}} \left(\frac{\rho l_i}{rl_i}\right)^{\bar{d}}$. Computing the i -th column of L^ρ requires the inversion of the Matrix Θ_{s_i, s_i} which can be done in computational complexity $C\rho^{3\bar{d}}$, leaving us with a total time complexity of $CN\rho^{\bar{d}}$. We now want to bound the computational complexity when using the aggregated sparsity patterns $\tilde{S}_{\prec, l, \rho, \lambda}$ or $\bar{S}_{\prec, l, \rho, \lambda}$. As before, we write $j \in s$ if j is a child of the supernode s , that is if there exists a $i \rightsquigarrow s$ such that (i, j) is contained in $\tilde{S}_{\prec, l, \rho, \lambda}$ or $\bar{S}_{\prec, l, \rho, \lambda}$. We write $\#s$ to denote the number of children of s . By the same argument as above, the number of *children* in each supernode s is bounded as $\#s \leq C\rho^{\bar{d}}$. We now want to show that the sum of the numbers of children of all supernodes is bounded as CN . For a supernode s we write $\sqrt{s} \in I$ to denote the index that was first added to the supernode (see the construction described in Section 3.2). We now observe that for two distinct supernodes s and t with $c \leq l_{\sqrt{s}}, l_{\sqrt{t}} \leq c\lambda$, we have $\text{dist}(x_{\sqrt{s}}, x_{\sqrt{t}}) \geq c\rho$, since otherwise we would have either $\sqrt{s} \rightsquigarrow t$ or $\sqrt{t} \rightsquigarrow s$. Thus, for every index $i \in I$ and $k \in \mathbb{Z}$, there exist at most C supernodes s with $i \in s$, $\lambda^k \leq l_{\sqrt{s}} < \lambda^{k+1}$. By using Condition 3.3, we thus obtain

$$\begin{aligned} \sum_{s \in \tilde{I}} \#s &= \sum_{i \in I} \#\{s \in \tilde{I} : i \in s\} = \sum_{k \in \mathbb{Z}} \sum_{i \in I} \#\{s \in \tilde{I} : i \in s, \lambda^k \leq l_{\sqrt{s}} < \lambda^{k+1}\} \\ &\leq \sum_{k \in \mathbb{Z}} \sum_{i \in I: l_i \geq \lambda^k} C \leq NC. \end{aligned}$$

We now know that there are at most CN child-parent relationships between indices and supernodes and that each supernode can have at most $C\rho^{\bar{d}}$ children. The worst case is thus that we have $CN/\rho^{\bar{d}}$ supernodes, each having $C\rho^{\bar{d}}$ children. This leads to the bounds on time- and space complexity of the algorithm. \square

C.2 Approximation accuracy

Schäfer et al. (2017) prove that under the conditions of Theorem 3.5 the Cholesky factor of $A = \Theta^{-1}$

decays exponentially away from the diagonal.

Theorem C.1 (Schäfer et al. (2017, Thm. 4.1)). *In the setting of Theorem 3.5, there exists a constant C depending only on $\delta, r, d, \Omega, s, \|\mathcal{L}\|$, and $\|\mathcal{L}^{-1}\|$, such that for $\rho \geq C \log(N/\epsilon)$,*

$$S \supset \{(i, j) \in I \times I : \text{dist}(x_i, x_j) \leq \rho \min(l_i, l_j)\}$$

and

$$L_{ij}^S := \begin{cases} (\text{chol}(A))_{ij}, & (i, j) \in S, \\ 0, & \text{otherwise,} \end{cases}$$

we have $\|A - L^S L^{S,\top}\|_{\text{FRO}} \leq \epsilon$.

In order to prove the approximation accuracy of the KL-minimizer, we have to compare the approximation accuracy in Frobenius norm and in KL-divergence.

Lemma C.2. *Let λ_{\min} , λ_{\max} be the minimal and maximal eigenvalues of Θ , respectively. Then there exists a universal constant C such that for any matrix $M \in \mathbb{R}^{I \times I}$, we have*

$$\begin{aligned} \lambda_{\max} \|A - MM^\top\|_{\text{FRO}} \leq C &\Rightarrow D_{\text{KL}}\left(\Theta \parallel (MM^\top)^{-1}\right) \leq \lambda_{\max} \|A - MM^\top\|_{\text{FRO}}, \text{ and} \\ D_{\text{KL}}\left(\Theta \parallel (MM^\top)^{-1}\right) \leq C &\Rightarrow \|A - MM^\top\|_{\text{FRO}} \leq \lambda_{\min}^{-1} D_{\text{KL}}\left(\Theta \parallel (MM^\top)^{-1}\right). \end{aligned}$$

Proof. Writing $L := \text{chol}(A)$ and $\phi_{\text{FRO}}(x) := x^2$ and $\phi_{\text{KL}}(x) := (x - \log(1+x))/2$, we have

$$\begin{aligned} \lambda_{\min} \|A - MM^\top\|_{\text{FRO}} &= \lambda_{\min} \|LL^{-1}(A - MM^\top)L^{-\top}L^\top\|_{\text{FRO}} \leq \|\text{Id} - L^{-1}MM^\top L^{-\top}\|_{\text{FRO}} \\ &= \sum_{k=1}^N \phi_{\text{FRO}}\left(\lambda_k\left(L^{-1}MM^\top L^{-\top}\right) - 1\right) = \|L^{-1}(A - MM^\top)L^{-\top}\|_{\text{FRO}} \leq \lambda_{\max} \|A - MM^\top\|_{\text{FRO}} \end{aligned}$$

and

$$D_{\text{KL}}\left(\Theta \parallel (MM^\top)^{-1}\right) = \sum_{k=1}^N \phi_{\text{KL}}\left(\lambda_k\left(L^{-1}MM^\top L^{-\top}\right)\right),$$

where $(\lambda_k(\cdot))_{1 \leq k \leq N}$ returns the eigenvalues ordered from largest to smallest, while $\lambda_{\min}(\cdot)$ ($\lambda_{\max}(\cdot)$) returns the smallest (largest) eigenvalue. The leading-order Taylor expansion of ϕ_{KL} around 0 is given by $x \mapsto x^2/4$. Thus, there exists a constant C such that for $\min(|x|, \phi_{\text{FRO}}(x), \phi_{\text{KL}}(x)) \leq C$ we have $\phi_{\text{KL}}(x) \leq \phi_{\text{FRO}}(x) \leq 8\phi_{\text{KL}}(x)$. Thus, for $\lambda_{\max} \|A - MM^\top\|_{\text{FRO}} \leq C$ we have $D_{\text{KL}}\left(\Theta \parallel (MM^\top)^{-1}\right) \leq \lambda_{\max} \|A - MM^\top\|_{\text{FRO}}$ and for $D_{\text{KL}}\left(\Theta \parallel (MM^\top)^{-1}\right) \leq C$, we obtain $\|A - MM^\top\|_{\text{FRO}} \leq \lambda_{\min}^{-1} D_{\text{KL}}\left(\Theta \parallel (MM^\top)^{-1}\right)$. \square

Using Lemma C.2, we can now use the results of Schäfer et al. (2017) to conclude Theorem 3.5.

Proof of Theorem 3.5. Schäfer et al. (2017, Thm. 3.16) implies that there exists a polynomial \mathbf{p} depending only on $(d, s, \delta, \mathcal{L})$ such that $\lambda_{\max}, \lambda_{\min}^{-1} \leq \mathbf{p}(N)$. Thus, by choosing $\rho \geq C \log(N)$ we can deduce by Theorem C.1 that $\lambda_{\max} \|A - L^S L^{S,\top}\| \leq C$ for C the constant in Lemma C.2.

Thus, We have $D_{\text{KL}}\left(\Theta \left\| \left(L^S L^{S,\top}\right)^{-1}\right.\right) \leq \lambda_{\max} \|A - L^S L^{S,\top}\|$. Using the KL-optimality of L^ρ as in Theorem 3.5, we deduce that $D_{\text{KL}}\left(\Theta \left\| \left(L^\rho L^{\rho,\top}\right)^{-1}\right.\right) \leq \lambda_{\max} \|A - L^S L^{S,\top}\| \leq C$. Using one more time Lemma C.2, we also obtain

$$\|A - L^\rho L^{\rho,\top}\| \leq \lambda_{\min}^{-1} D_{\text{KL}}\left(\Theta \left\| \left(L^\rho L^{\rho,\top}\right)^{-1}\right.\right) \leq \lambda_{\max}/\lambda_{\min} \|A - L^S L^{S,\top}\|.$$

□

D Including the prediction points

D.1 Ordering the prediction points first

Algorithm 11 describes how to compute the inverse Cholesky factor when forcing the prediction points to be ordered before the training points. In order to compute the ordering of the prediction points after the ordering of the training points has been fixed, we need to compute the distance of each prediction point to the closest training point. When using Schäfer et al. (2017, Alg. 3), this can be done efficiently while computing the maximin ordering of the training points by including the prediction points into the initial list of children of i , as is done in Line 11 of the algorithm. Once the joint inverse Cholesky factor $L = \begin{pmatrix} L_{\text{Pr},\text{Pr}} & 0 \\ L_{\text{Tr},\text{Pr}} & L_{\text{Tr},\text{Tr}} \end{pmatrix}$ has been computed, we have $\mathbb{E}[X_{\text{Pr}}|X_{\text{Tr}} = y] = L_{\text{Pr},\text{Pr}}^{-\top} L_{\text{Tr},\text{Pr}}^\top y$ and $\text{Cov}[X_{\text{Pr}}|X_{\text{Tr}}] = L_{\text{Pr},\text{Pr}}^{-\top} L_{\text{Pr},\text{Pr}}^{-1}$. We note that the conditional expectation can be computed by forming the columns of L one by one, without every having to hold the entire matrix in memory, thus leading to linear space complexity similar to Section 4.2, while the same is not possible for the conditional covariance matrix.

D.2 Ordering the prediction points last, for accurate extrapolation

Splitting the prediction set $I_{\text{Pr}} = \bigcup_{1 \leq b \leq m_{\text{Pr}}} J_b$ into m_{Pr} batches of n_{Pr} predictions, we want to compute the conditional mean vector and covariance matrix of the variables in each batch separately, by using the inverse Cholesky factor \bar{L}^ρ of the joint covariance matrix obtained from KL-minimization subject to the sparsity constraint given by $\bar{S} = S_{\prec, l, \rho, \lambda} \cup \{(i, j) : j \in J_b\}$. Naively, this requires us to recompute the inverse Cholesky factor L for every batch, leading to a computational complexity of $\mathcal{O}\left(m_{\text{Pr}}(N + n_{\text{Pr}})(\rho^{\bar{d}} + n_{\text{Pr}})^2\right)$. However, by reusing a part of the computational complexity across different batches, Algorithm 13 is to instead achieve computational complexity of $\mathcal{O}\left((N + n_{\text{Pr}})(\rho^{2\bar{d}} + m_{\text{Pr}}(\rho^{\bar{d}} + n_{\text{Pr}}^2))\right)$. In the following, we derive the formulae used by this algorithm to compute the conditional mean and covariance. For a fixed batch J_b , define $\bar{\Theta}$ as the approximate joint covariance matrix implied by the inverse Cholesky factor \bar{L}^ρ . It has the block-structure

$$\bar{\Theta} = \begin{pmatrix} \bar{\Theta}_{\text{Tr},\text{Tr}} & \bar{\Theta}_{\text{Tr},b} \\ \bar{\Theta}_{b,\text{Tr}} & \bar{\Theta}_{b,b} \end{pmatrix} =: \begin{pmatrix} \bar{A}_{\text{Tr},\text{Tr}} & \bar{A}_{\text{Tr},b} \\ \bar{A}_{b,\text{Tr}} & \bar{A}_{b,b} \end{pmatrix}^{-1} = \begin{pmatrix} \bar{L}_{\text{Tr},\text{Tr}}^\top & \bar{L}_{b,\text{Tr}}^\top \\ 0 & \bar{L}_{b,b}^\top \end{pmatrix}^{-1} \begin{pmatrix} \bar{L}_{\text{Tr},\text{Tr}} & 0 \\ \bar{L}_{b,\text{Tr}} & \bar{L}_{b,b} \end{pmatrix}^{-1} =: \bar{L}^{\rho,-\top} \bar{L}^{\rho,-1},$$

where \bar{L}^ρ is the inverse-Cholesky factor obtained by applying KL-minimization to the joint covariance matrix subject to the sparsity constraint given by \bar{S} . We can then write the posterior mean and covariance of a GP $X \sim \mathcal{N}(0, \bar{\Theta})$ as

$$\mathbb{E}[X_b|X_{\text{Tr}} = y] = \bar{\Theta}_{b,\text{Tr}} \bar{\Theta}_{\text{Tr},\text{Tr}}^{-1} y = -\bar{A}_{b,b}^{-1} \bar{A}_{b,\text{Tr}} y = -\left(\bar{L}_{b,\text{Tr}} \bar{L}_{b,\text{Tr}}^\top + \bar{L}_{b,b} \bar{L}_{b,b}^\top\right)^{-1} \bar{L}_{b,\text{Tr}} \bar{L}_{\text{Tr},\text{Tr}}^\top y$$

$$\text{Cov}[X_b|X_{\text{Tr}}] = \bar{\Theta}_{b,b} - \bar{\Theta}_{b,\text{Tr}}\bar{\Theta}_{\text{Tr},\text{Tr}}^{-1}\bar{\Theta}_{\text{Tr},b} = \bar{A}_{b,b}^{-1} = \left(\bar{L}_{b,\text{Tr}}\bar{L}_{b,\text{Tr}}^\top + \bar{L}_{b,b}\bar{L}_{b,b}^\top\right)^{-1}$$

Expanding the matrix multiplications into sums, this can be rewritten as

$$\begin{aligned} \mathbb{E}[X_b|X_{\text{Tr}}] &= - \left(\bar{L}_{b,b}\bar{L}_{b,b}^\top + \sum_{k \in I_{\text{Tr}}} \bar{L}_{b,k} \otimes \bar{L}_{b,k} \right)^{-1} \sum_{k \in I_{\text{Tr}}} \bar{L}_{b,k} \left(y^\top \bar{L}_{\text{Tr},k} \right). \\ \text{Cov}[X_b|X_{\text{Tr}}] &= \left(\bar{L}_{b,b}\bar{L}_{b,b}^\top + \sum_{k \in I_{\text{Tr}}} \bar{L}_{b,k} \otimes \bar{L}_{b,k} \right)^{-1} \end{aligned}$$

$\bar{L}_{b,b}$ is simply the Cholesky factor of $\Theta_{b,b}^{-1}$. Thus, given $(y^\top \bar{L}_{\text{Tr},k}, L_{b,k})_{k \rightsquigarrow \tilde{k}}$, the above expressions can be evaluated in computational complexity $\mathcal{O}(n_{\text{Pr}}^3 + N_{\text{Tr}}n_{\text{Pr}}^2 + n_{\text{Pr}}\#S)$ in time and $\mathcal{O}(n_{\text{Pr}}^2 + \max_{\tilde{l} \in \tilde{I}_k} \#\tilde{l})$ in space. Naively, computing the $(y^\top L_{\text{Tr},k}, L_{b,k})_{k \rightsquigarrow \tilde{k}}$ for each batch has computational complexity $\mathcal{O}(m_{\text{Pr}}(\#\tilde{k} + n_{\text{Pr}})^3)$ which becomes the bottleneck for large numbers of batches. However, as we will see, $\langle L_{\text{Tr},k}, y \rangle$ and $L_{b,k}$ can be computed in computational complexity $\mathcal{O}((\#\tilde{k} + n_{\text{Pr}})^3 + m_{\text{Pr}}(\#\tilde{k} + n_{\text{Pr}})^2)$ by reusing parts of the computation. Fix a supernodal index $\tilde{k} \in \tilde{I}$ and define the corresponding exact joint covariance matrix as

$$\Theta^{\tilde{k}} := (\Theta_{ij})_{\{i,j \in \tilde{k} \cup J_b\}} = \begin{pmatrix} \Theta_{\tilde{k},\tilde{k}} & \Theta_{\tilde{k},b} \\ \Theta_{b,\tilde{k}} & \Theta_{b,b} \end{pmatrix}$$

For any $k \rightsquigarrow \tilde{k}$ the column $L_{:,k}^\rho$ is, according to Equation 2.3, equal to

$$\frac{\left(\Theta_{k:,k}^{\tilde{k}}\right)^{-1} \mathbf{e}_1}{\sqrt{\mathbf{e}_1^\top \left(\Theta_{k:,k}^{\tilde{k}}\right)^{-1} \mathbf{e}_1}}.$$

Let as before $U^{\tilde{k}}U^{\tilde{k},\top} = \Theta_{\tilde{k},\tilde{k}}$. Using the Sherman-Morrison-Woodbury matrix identity we can then rewrite $\Theta_{k:,k}^{\tilde{k},-1} \mathbf{e}_1$ as

$$\begin{aligned} \Theta_{k:,k}^{\tilde{k},-1} \mathbf{e}_1 &= \begin{pmatrix} \text{Id} & 0 \\ -\Theta_{b,b}^{-1}\Theta_{b,s_k} & \text{Id} \end{pmatrix} \begin{pmatrix} \left(\Theta_{s_k,s_k} - \Theta_{s_k,b}\Theta_{b,b}^{-1}\Theta_{b,s_k}\right)^{-1} & 0 \\ 0 & \Theta_{b,b}^{-1} \end{pmatrix} \begin{pmatrix} \text{Id} & -\Theta_{s_k,b}\Theta_{b,b}^{-1} \\ 0 & \text{Id} \end{pmatrix} \mathbf{e}_1 \\ &= \begin{pmatrix} \left(\Theta_{s_k,s_k} - \Theta_{s_k,b}\Theta_{b,b}^{-1}\Theta_{b,s_k}\right)^{-1} \mathbf{e}_1 \\ -\Theta_{b,b}^{-1}\Theta_{b,s_k} \left(\Theta_{s_k,s_k} - \Theta_{s_k,b}\Theta_{b,b}^{-1}\Theta_{b,s_k}\right)^{-1} \mathbf{e}_1 \end{pmatrix} \\ &= \begin{pmatrix} \left(\Theta_{s_k,s_k}^{-1} - \Theta_{s_k,s_k}^{-1}\Theta_{s_k,b}(-\Theta_{b,b} + \Theta_{b,s_k}\Theta_{s_k,s_k}^{-1}\Theta_{s_k,b})^{-1}\Theta_{b,s_k}\Theta_{s_k,s_k}^{-1}\right) \mathbf{e}_1 \\ -\Theta_{b,b}^{-1}\Theta_{b,s_k} \left(\Theta_{s_k,s_k}^{-1} - \Theta_{s_k,s_k}^{-1}\Theta_{s_k,b}(-\Theta_{b,b} + \Theta_{b,s_k}\Theta_{s_k,s_k}^{-1}\Theta_{s_k,b})^{-1}\Theta_{b,s_k}\Theta_{s_k,s_k}^{-1}\right) \mathbf{e}_1 \end{pmatrix} \end{aligned}$$

Using Equation (A.1) and setting $B^{\tilde{k}} := U^{\tilde{k},-1}\Theta_{\tilde{k},b}$, we obtain

$$\Theta_{k:,k}^{\tilde{k},-1} \mathbf{e}_1 = \frac{1}{U_{k,k}^{\tilde{k}}} \begin{pmatrix} U_{s_k,s_k}^{\tilde{k},\top} \left(\mathbf{e}_1 + B_{s_k,b}^{\tilde{k}} \left(\Theta_{b,b} - B_{s_k,b}^{\tilde{k},\top} B_{s_k,b}^{\tilde{k}} \right)^{-1} B_{k,b}^{\tilde{k},\top} \right) \\ -\Theta_{b,b}^{-1} B_{s_k,b}^{\tilde{k},\top} \left(\mathbf{e}_1 + B_{s_k,b}^{\tilde{k}} \left(\Theta_{b,b} - B_{s_k,b}^{\tilde{k},\top} B_{s_k,b}^{\tilde{k}} \right)^{-1} B_{k,b}^{\tilde{k},\top} \right) \end{pmatrix}.$$

Setting $y^{\tilde{k}} = U^{\tilde{k},-1}y_{s_{\tilde{k}}}$, this yields the formulae

$$y^\top \bar{L}_{\text{Tr},k} = \frac{y_k^{\tilde{k},\top} + y_{s_k}^{\tilde{k},\top} B_{s_k,b}^{\tilde{k}} \left(\Theta_{b,b} - B_{s_k,b}^{\tilde{k},\top} B_{s_k,b}^{\tilde{k}} \right)^{-1} B_{k,b}^{\tilde{k},\top}}{c_k}$$

$$\bar{L}_{b,k} = \frac{-\Theta_{b,b}^{-1} B_{s_k,b}^{\tilde{k},\top} \left(\mathbf{e}_1 + B_{s_k,b}^{\tilde{k}} \left(\Theta_{b,b} - B_{s_k,b}^{\tilde{k},\top} B_{s_k,b}^{\tilde{k}} \right)^{-1} B_{k,b}^{\tilde{k},\top} \right)}{c_k},$$

where

$$c_k := \sqrt{1 + B_{k,b}^{\tilde{k}} \left(\Theta_{b,b} - B_{s_k,b}^{\tilde{k},\top} B_{s_k,b}^{\tilde{k}} \right)^{-1} B_{k,b}^{\tilde{k},\top}}.$$

Algorithm 13 implements the formulae above. Since $U^{\tilde{k}}$ does not depend on b , it only has to be computed once and can be used to compute the $B^{\tilde{k}}$ and $y^{\tilde{y}}$ for all $1 \leq b \leq m_{\text{Pr}}$.

Algorithm 7: Ordering and sparsity pattern algorithm (see Schäfer et al. (2017, Alg. 3)).

Data: A real parameter $\rho \geq 2$ and Oracles $\text{dist}(\cdot, \cdot)$, $\text{dist}_{\partial\Omega}(\cdot)$ such that $\text{dist}(i, j) = \text{dist}(x_i, x_j)$ and $\text{dist}_{\partial\Omega}(i) = \text{dist}(x_i, \partial\Omega)$

Result: An array $l[\cdot]$ of distances, an array P encoding the multiresolution ordering, and an array of index pairs S containing the sparsity pattern.

```

1  $P = \emptyset$ ;
2 for  $i \in \{1, \dots, N\}$  do
3    $l[i] \leftarrow \text{dist}_{\partial\Omega}(i)$ ;
4    $p[i] \leftarrow \emptyset$ ;
5    $c[i] \leftarrow \emptyset$ ;

  /* Creates a mutable binary heap, containing pairs of indices and distances as elements: */
6  $H \leftarrow \text{MutableMaximalBinaryHeap}(\{(i, l[i])\}_{i \in \{1, \dots, N\}})$ ;
  /* Instates the Heap property, with a pair with maximal distance occupying the root of the
   heap: */
7  $\text{heapSort!}(H)$ ;
  /* Processing the first index: */
  /* Get the root of the heap, remove it, and restore the heap property: */
8  $(i, l) = \text{pop}(H)$ ;
  /* Add the index as the next element of the ordering */
9  $\text{push}(P, i)$ ;
10 for  $j \in \{1, \dots, N\}$  do
11    $\text{push}(c[i], j)$ ;
12    $\text{push}(p[j], i)$ ;
13    $\text{sort!}(c[i], \text{dist}(\cdot, i))$ ;
14    $\text{decrease!}(H, j, \text{dist}(i, j))$ ;

  /* Processing remaining indices: */
15  $l_{\text{Trunc}} \leftarrow l$  while  $H \neq \emptyset$  do
  /* Get the root of the heap, remove it, and restore the heap property: */
16  $(i, l) = \text{pop}(H)$ ;
17  $l[i] \leftarrow l$ ;
  /* Select the parent node that has all possible children of  $i$  amongst its children, and is
   closest to  $i$ : */
18  $k = \text{argmin}_{j \in p[i]: \text{dist}(i, j) + \rho l[i] \leq \rho \min(l_{\text{Trunc}}, l[j])} \text{dist}(i, j)$ ;
  /* Loop through those children of  $k$  that are close enough to  $k$  to possibly be children of
    $i$ : */
19 for  $j \in c[k] : \text{dist}(j, k) \leq \text{dist}(i, k) + \rho l[i]$  do
20    $\text{decrease!}(H, j, \text{dist}(i, j))$ ;
21   if  $\text{dist}(i, j) \leq \rho l[i]$  then
22      $\text{push}(c[i], j)$ ;
23      $\text{push}(p[j], i)$ ;

  /* Add the index as the next element of the ordering */
24  $\text{push}(P, i)$ ;
  /* Sort the children according to distance to the parent node, so that the closest
   children can be found more easily */
25  $\text{sort!}(c[i], \text{dist}(\cdot, i))$ ;
  /* Truncate the sparsity pattern to achieve linear space complexity */
26 if  $\forall j \notin P, \exists i \in P : \text{dist}(i, j) < l_{\text{Trunc}}/2$  then
27    $l_{\text{Trunc}} \leftarrow l_{\text{Trunc}}/2$ ;
28   for  $j \in c[i] \setminus P, \text{dist}(i, j) > \rho l_{\text{Trunc}}$  do
29      $c[i] \leftarrow c[i] \setminus \{j\}$ ;
30      $p[j] \leftarrow p[j] \setminus \{i\}$ ;

  /* Aggregating the lists of children into the sparsity pattern: */
31 for  $i \in \{1, \dots, N\}$  do
32   for  $j \in c[i]$  do
33      $\text{push!}(S, (i, j))$ ;
34      $\text{push!}(S, (j, j))$ ;

```

Algorithm 8: Computation of \tilde{S} and \bar{S}

Data: $I, \prec, l, \text{dist}(\cdot, \cdot), \rho, \lambda$
Result: Sets of supernodes \bar{S}, \tilde{S}

$i_N, i_{N-1} \leftarrow$ the last two indices w.r.t. \prec ;
 $\mathcal{N}, \mathcal{N}^\geq \leftarrow \{(\{i_N\}, I), (\{i_N\}, \{i_N\})\}$;
 $r, l_{i_N} \leftarrow l_{i_{N-1}}/\lambda, \infty$;

while $r > \min_{i \in I} l_i$ **do**
 $\mathcal{N}, \tilde{\mathcal{N}}^\geq \leftarrow \text{Refine}(\mathcal{N}, \prec, l, r, \rho, \lambda)$;
 $\mathcal{N}^\geq \leftarrow \mathcal{N}^\geq \cup \tilde{\mathcal{N}}^\geq$;
 $n \leftarrow n + 1$;
 $r \leftarrow r/\lambda$

$J, \bar{S} \leftarrow \emptyset, \emptyset$;
for $i \in I$ (in increasing order by \prec) **do**
 if $i \notin J$ **then**
 $\bar{s} = (\emptyset, \emptyset)$;
 Pick any $\sigma \in \mathcal{N}^\geq$ such that $i \in \sigma_m$;
 for $j \in \sigma_m$ **do**
 if $i \preceq j, l_j \leq \lambda l_i, j \notin J$ **then**
 $J, \bar{s}_n \leftarrow J \cup \{j\}, \bar{s}_n \cup \{j\}$;
 for $\bar{\sigma} \in \mathcal{N}^\geq : \exists j \in \bar{\sigma}_m : j \in \sigma_m$ **do**
 for $k \in \bar{\sigma}_n : \text{dist}(i, k) \leq \rho(1 + \lambda)$ **do**
 $\bar{s}_m \leftarrow \bar{s}_m \cup \{k\}$;
 $\bar{S} \leftarrow \bar{S} \cup \{\bar{s}\}$;

$\tilde{S} \leftarrow \text{Reduce}(\rho, \prec, l, \bar{S})$;
return \bar{S}, \tilde{S} ;

Algorithm 9: $\text{Reduce}(\rho, \prec, l, \bar{S})$

Data: $\prec, l, \text{dist}(\cdot, \cdot), \rho, \bar{S}$
Result: $\tilde{S} = \tilde{S}_{\prec, l, \rho}$

$\tilde{S} \leftarrow \emptyset$;
for $\sigma \in \bar{S}$ **do**
 $\bar{s} \leftarrow (\sigma_m, \emptyset)$;
 for $i \in \sigma_m, j \in \sigma_n$ **do**
 if $\text{dist}(i, j) \leq \rho l_i$ and $i \prec j$ **then**
 $\bar{s}_n \leftarrow \bar{s}_n \cup \{j\}$;
 $\tilde{S} \leftarrow \tilde{S} \cup \{\bar{s}\}$;

return \tilde{S} ;

Algorithm 10: $\text{Refine}(\mathcal{N}, \prec, l, r, \rho, \lambda)$

Data: Supernodal set $\mathcal{N}, \text{dist}(\cdot, \cdot), \prec, l, r, \rho, \lambda$
Result: A new set \mathcal{M} of supernodes, set \mathcal{N}^\geq of truncated supernodes

$J, \mathcal{N}^\geq, \mathcal{M} \leftarrow \emptyset, \emptyset, \emptyset$;
while $J \neq I$ **do**
 Pick $i \in I \setminus J$;
 $J \leftarrow J \cup \{i\}$;
 Pick the $\sigma \in \mathcal{N}$ that satisfies $i \in \sigma_m$;
 $\bar{\sigma}_m, \bar{\sigma}_n \leftarrow \emptyset, \emptyset$;
 for $j \in \sigma_n$ **do**
 if $\text{dist}(i, j) \leq \rho \lambda r$ **then**
 $\bar{\sigma}_m \leftarrow \bar{\sigma}_m \cup \{j\}$;
 $J \leftarrow J \cup \{j\}$
 if $\text{dist}(i, j) \leq 2\rho \lambda r$ **then**
 $\bar{\sigma}_n \leftarrow \bar{\sigma}_n \cup \{j\}$;
 $\mathcal{M} \leftarrow \mathcal{M} \cup \{(\bar{\sigma}_m, \bar{\sigma}_n)\}$;

for $\sigma \in \mathcal{N}$ **do**
 $\sigma_m^\geq, \sigma_n^\geq \leftarrow \emptyset, \emptyset$;
 for $i \in \sigma_m$ **do**
 if $r \leq l_i$ **then**
 $\sigma_m^\geq \leftarrow \sigma_m^\geq \cup \{i\}$
 for $i \in \sigma_n$ **do**
 if $r \leq l_i$ **then**
 $\sigma_n^\geq \leftarrow \sigma_n^\geq \cup \{i\}$
 $\mathcal{N}^\geq \leftarrow \mathcal{N}^\geq \cup \{(\sigma_m^\geq, \sigma_n^\geq)\}$

return $\mathcal{M}, \mathcal{N}^\geq$;

Figure 12: Algorithm for constructing the aggregated sparsity pattern from the reverse maximin ordering \prec and length-scales l

Algorithm 11: Ordering prediction variables first, for rapid interpolation

Data: $G, \{x_i\}_{i \in I_{\text{Tr}}}, \Omega, \{x_i\}_{i \in I_{\text{Pr}}}, \rho, (\lambda)$
Result: $L \in \mathbb{R}^{N \times N}$ lower triangular in \prec
Compute $\prec_{\text{Pr}}, l_{\text{Pr}}$ from $\{x_i\}_{i \in I_{\text{Pr}}}, \tilde{\Omega}$;
Compute $\prec_{\text{Tr}}, l_{\text{Tr}}$ from $\{x_i\}_{i \in I_{\text{Tr}}}, \Omega$;
 $\prec \leftarrow (\prec_{\text{Pr}}, \prec_{\text{Tr}})$;
 $l \leftarrow (l_{\text{Pr}}, l_{\text{Tr}})$;
 $S \leftarrow S_{\prec, l, \rho}$ ($S \leftarrow S_{\prec, l, \rho, \lambda}$);
Compute L using Algorithm 1(2);
return L ;

Algorithm 12: Ordering prediction variables last, with $n_{\text{Pr}} = 1$

Data: $G, \{x_i\}_{i \in I_{\text{Tr}}}, \Omega, \{x_i\}_{i \in I_{\text{Pr}}}, \rho, \lambda$
Result: Cond. mean and variance $\mu, \sigma \in \mathbb{R}^{I_{\text{Pr}}}$
Compute $\prec, S_{\prec, l, \rho, \lambda}$ from $\{x_i\}_{i \in I_{\text{Tr}}}, \Omega$;
for $k \in I_{\text{Pr}}$ **do**
 $\delta_k, \sigma_k \leftarrow G(x_k, x_k), G(x_k, x_k)^{-1}$;
 $\mu_k \leftarrow 0$;
for $\tilde{k} \in \tilde{I}$ **do**
 $U \leftarrow P^\dagger \text{chol}(P^\dagger \Theta_{s_{\tilde{k}}, s_{\tilde{k}}} P^\dagger) P^\dagger$;
 for $k \in s_{\tilde{k}}, l \in I_{\text{Pr}}$ **do**
 $B_{kl} \leftarrow G(x_k, x_l)$;
 $B \leftarrow U^{-1} B$;
 $\tilde{y} \leftarrow U^{-1} y_{s_{\tilde{k}}}$;
 for $k \rightsquigarrow \tilde{k}$ **do**
 $\alpha \leftarrow \tilde{y}_{s_k}^\top B_{s_k, \text{Pr}}$;
 $\beta \leftarrow B_{s_k, \text{Pr}}^\top B_{s_k, \text{Pr}}$;
 $\gamma \leftarrow \sqrt{1 + (\delta - \beta)^{-1} B_{k, \text{Pr}}^2}$;
 $\ell \leftarrow -\delta^{-1} \gamma^{-1} B_{k, \text{Pr}}^\top (1 + \beta / (\delta - \beta))$;
 $\mu \leftarrow \mu + \ell / \gamma (\tilde{y}_k + B_{k, \text{Pr}} \alpha / (\delta - \beta))$;
 $\sigma \leftarrow \sigma + \ell^2$;
 $\sigma \leftarrow \sigma^{-1}$;
 $\mu \leftarrow -\sigma \mu$;
return μ, σ ;

Algorithm 13: Ordering prediction variables last, for accurate extrapolation

Data: $G, \{x_i\}_{i \in I_{\text{Tr}}}, \Omega, \{x_i\}_{i \in I_{\text{Pr}}}, \rho, \lambda$
Result: Per batch cond. mean $\{\mu_b\}_{1 \leq b \leq m_{\text{Pr}}}$ and covariance $\{C_b\}_{1 \leq b \leq m_{\text{Pr}}}$
Compute $\prec, S_{\prec, l, \rho, \lambda}$ from $\{x_i\}_{i \in I_{\text{Tr}}}, \Omega$;
for $\tilde{k} \in \tilde{I}$ **do**
 $U^{\tilde{k}} \leftarrow P^\dagger \text{chol}(P^\dagger \Theta_{s_{\tilde{k}}, s_{\tilde{k}}} P^\dagger) P^\dagger$;
for $b \in \{1, \dots, m_{\text{Pr}}\}$ **do**
 for $\tilde{k} \in \tilde{I}$ **do**
 for $k \in s_{\tilde{k}}, l \in J_b$ **do**
 $(\Theta_{s_{\tilde{k}}, b})_{kl} \leftarrow G(x_k, x_l)$;
 for $k, l \in J_b$ **do**
 $(\Theta_{b, b})_{kl} \leftarrow G(x_k, x_l)$;
 $C_b \leftarrow \Theta_{b, b}^{-1}$;
 $B^{\tilde{k}} \leftarrow U^{\tilde{k}, -1} \Theta_{\tilde{k}, b}$;
 $y^{\tilde{k}} \leftarrow U^{\tilde{k}, -1} y_{s_{\tilde{k}}}$;
 for $k \rightsquigarrow \tilde{k}$ **do**
 $v \leftarrow B_{s_k, b}^{\tilde{k}} \left(\Theta_{b, b} - B_{s_k, b}^{\tilde{k}, \top} B_{s_k, b} \right)^{-1} B_{k, b}^{\tilde{k}, \top}$;
 $c \leftarrow \sqrt{1 + v_k}$;
 $L_{b, k} \leftarrow -\frac{1}{c_k} \Theta_{b, b}^{-1} B_{s_k, b}^{\tilde{k}, \top} (\mathbf{e}_1 + v)$;
 $C_b \leftarrow C_b + L_{b, k} L_{b, k}^\top$;
 $\mu_b \leftarrow \mu_b + L_{b, k} \left(\frac{1}{c_k} y_{s_k}^{\tilde{k}, \top} (\mathbf{e}_1 + v) \right)$;
 $\mu_b \leftarrow -C_b \mu_b$;
 $C_b \leftarrow C_b^{-1}$;
return $(\mu_b, C_b)_{1 \leq b \leq m_{\text{Pr}}}$;

Figure 13: The algorithms to use when ordering prediction points first or last. Here, we partition the prediction variables into batches, as $I_{\text{Pr}} = \bigcup_{b=1}^{m_{\text{Pr}}} J_b$.